

Fluoride-Salt-Cooled High-Temperature Reactor Generative Design Optimization with Evolutionary Algorithms

Ph.D. Defense

Gwendolyn J.Y. Chee

Dept. of Nuclear, Plasma and Radiological Engineering
University of Illinois at Urbana-Champaign

August 12, 2022



ILLINOIS



Outline

① Introduction

Overview

Background: Advanced High Temperature Reactor

Objectives: AHTR Model Development

Background: Generative Reactor Design Optimization

Objectives: AHTR Optimization for Non-Conventional Designs

Summary

② FHR Benchmark Results

FHR Benchmark Specifications

FHR Benchmark Results

③ AHTR Temperature Model Verification and Results

AHTR Temperature Model with Moltres

Key Neutronics Parameters Verification

AHTR Temperature Model Results

Summary

④ ROLLO: Reactor evOLutionary aLgorithm Optimizer

ROLLO: Reactor evOLutionary aLgorithm Optimizer

⑤ AHTR Optimization for Non-Conventional Designs

Optimization Methodology

AHTR One-Third Assembly Optimization Results

⑥ Conclusion

Conclusion

Future Work

Introduction

FHR Benchmark Results

AHTR Temperature Model Verification and Results

ROLLO: Reactor evOLutionary aLgorithm Optimizer

AHTR Optimization for Non-Conventional Designs

Conclusion

Overview

Background: Advanced High Temperature Reactor

Objectives: AHTR Model Development

Background: Generative Reactor Design Optimization

Objectives: AHTR Optimization for Non-Conventional Designs

Summary

Introduction

FHR Benchmark Results

AHTR Temperature Model Verification and Results

ROLLO: Reactor evOLutionary aLgorithm Optimizer

AHTR Optimization for Non-Conventional Designs

Conclusion

Overview

Background: Advanced High Temperature Reactor

Objectives: AHTR Model Development

Background: Generative Reactor Design Optimization

Objectives: AHTR Optimization for Non-Conventional Designs

Summary

Overview



In this defense, I will show that I successfully:

Introduction

FHR Benchmark Results

AHTR Temperature Model Verification and Results

ROLLO: Reactor evOLutionary aLgorithm Optimizer

AHTR Optimization for Non-Conventional Designs

Conclusion

Overview

Background: Advanced High Temperature Reactor

Objectives: AHTR Model Development

Background: Generative Reactor Design Optimization

Objectives: AHTR Optimization for Non-Conventional Designs

Summary

Overview



In this defense, I will show that I successfully:

- ① Furthered our understanding of the AHTR design's complexities through neutronics and temperature modeling

Introduction

FHR Benchmark Results

AHTR Temperature Model Verification and Results

ROLLO: Reactor evOLutionary aLgorithm Optimizer

AHTR Optimization for Non-Conventional Designs

Conclusion

Overview

Background: Advanced High Temperature Reactor

Objectives: AHTR Model Development

Background: Generative Reactor Design Optimization

Objectives: AHTR Optimization for Non-Conventional Designs

Summary

Overview



In this defense, I will show that I successfully:

- ① Furthered our understanding of the AHTR design's complexities through neutronics and temperature modeling
- ② Created an open-source tool that enables reactor generative design optimization with evolutionary algorithms

Introduction

FHR Benchmark Results

AHTR Temperature Model Verification and Results

ROLLO: Reactor evOLutionary aLgorithm Optimizer

AHTR Optimization for Non-Conventional Designs

Conclusion

Overview

Background: Advanced High Temperature Reactor

Objectives: AHTR Model Development

Background: Generative Reactor Design Optimization

Objectives: AHTR Optimization for Non-Conventional Designs

Summary

Overview



In this defense, I will show that I successfully:

- ① Furthered our understanding of the AHTR design's complexities through neutronics and temperature modeling
- ② Created an open-source tool that enables reactor generative design optimization with evolutionary algorithms
- ③ Applied the optimization tool to the AHTR design for non-conventional geometries and fuel distributions

Introduction

FHR Benchmark Results

AHTR Temperature Model Verification and Results

ROLLO: Reactor evOLutionary aLgorithm Optimizer

AHTR Optimization for Non-Conventional Designs

Conclusion

Overview

Background: Advanced High Temperature Reactor

Objectives: AHTR Model Development

Background: Generative Reactor Design Optimization

Objectives: AHTR Optimization for Non-Conventional Designs

Summary

MSR + VHTR = FHR



Gen IV Forum identified **new and innovative Gen IV nuclear energy systems:**
Molten Salt Reactors (MSR) and Very High-Temperature Reactors (VHTR).

Introduction

FHR Benchmark Results

AHTR Temperature Model Verification and Results

ROLLO: Reactor evOLutionary aLgorithm Optimizer

AHTR Optimization for Non-Conventional Designs

Conclusion

Overview

Background: Advanced High Temperature Reactor

Objectives: AHTR Model Development

Background: Generative Reactor Design Optimization

Objectives: AHTR Optimization for Non-Conventional Designs

Summary

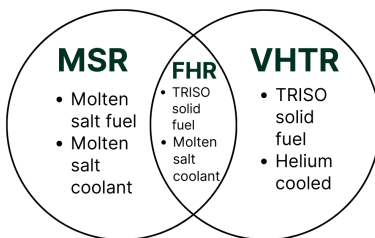
$$\text{MSR} + \text{VHTR} = \text{FHR}$$



Gen IV Forum identified **new and innovative Gen IV nuclear energy systems:**
Molten Salt Reactors (MSR) and Very High-Temperature Reactors (VHTR).

The **Fluoride-Salt Cooled**
High-Temperature Reactor (FHR)
concept combines the best aspects of
MSR and VHTR.

The Advanced High-Temperature
Reactor (AHTR) is a subset of the FHR.



Introduction

FHR Benchmark Results

AHTR Temperature Model Verification and Results

ROLLO: Reactor eVOLutionary aLgorithm Optimizer

AHTR Optimization for Non-Conventional Designs

Conclusion

Overview

Background: Advanced High Temperature Reactor

Objectives: AHTR Model Development

Background: Generative Reactor Design Optimization

Objectives: AHTR Optimization for Non-Conventional Designs

Summary

$$\text{MSR} + \text{VHTR} = \text{FHR}$$



Gen IV Forum identified **new and innovative Gen IV nuclear energy systems:**
Molten Salt Reactors (MSR) and Very High-Temperature Reactors (VHTR).

The **Fluoride-Salt Cooled
High-Temperature Reactor (FHR)**
concept combines the best aspects of
MSR and VHTR.

The Advanced High-Temperature
Reactor (AHTR) is a subset of the FHR.

Fluoride-Lithium-Beryllium (FLiBe) salt
cooled: **superior cooling, low
operating pressure**

Tristructural Isotropic (TRISO) fuel:
fuel kernel encapsulated in three other
layers, **extra barriers to fission product
release, higher safety margin**

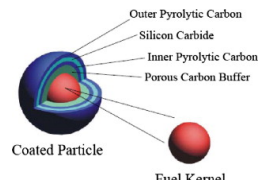
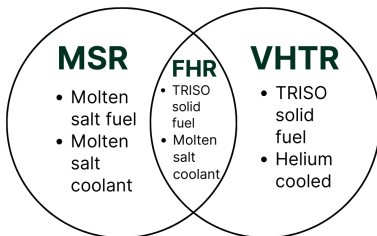


Figure 1: TRISO diameter $\approx 8\text{mm}$.

Introduction

FHR Benchmark Results

AHTR Temperature Model Verification and Results

ROLLO: Reactor evOLutionary aLgorithm Optimizer

AHTR Optimization for Non-Conventional Designs

Conclusion

Overview

Background: Advanced High Temperature Reactor

Objectives: AHTR Model Development

Background: Generative Reactor Design Optimization

Objectives: AHTR Optimization for Non-Conventional Designs

Summary

Advanced High Temperature Reactor Design



- Design developed by Oak Ridge National Laboratory
- Prismatic FHR design with 252 hexagonal fuel assemblies consisting of 18 fuel planks arranged in 3 diamond-shaped sectors

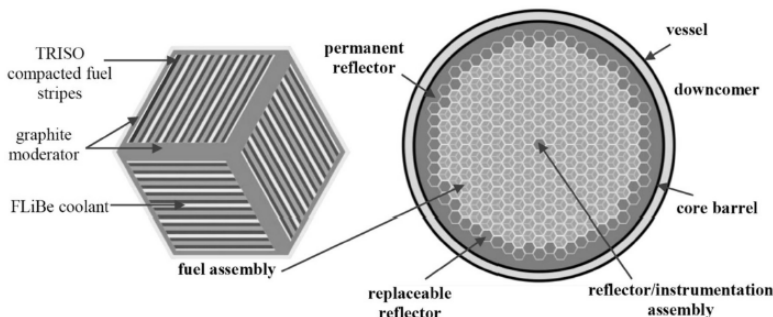


Figure 2: Advanced High-Temperature Reactor full assembly (left) and core configuration (right) reproduced from [1].

Introduction

FHR Benchmark Results

AHTR Temperature Model Verification and Results

ROLLO: Reactor evOLutionary aLgorithm Optimizer

AHTR Optimization for Non-Conventional Designs

Conclusion

Overview

Background: Advanced High Temperature Reactor

Objectives: AHTR Model Development

Background: Generative Reactor Design Optimization

Objectives: AHTR Optimization for Non-Conventional Designs

Summary

Advanced High Temperature Reactor Geometry

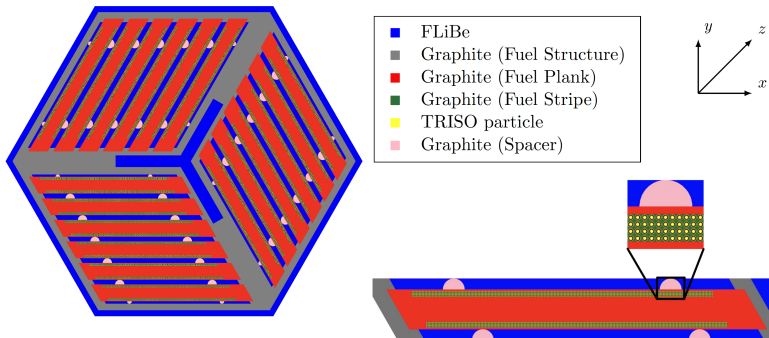


Figure 3: AHTR full assembly with 18 fuel plates arranged in three diamond-shaped sectors, with a central Y-shaped and external channel graphite structure.

Introduction

FHR Benchmark Results

AHTR Temperature Model Verification and Results

ROLLO: Reactor evOLutionary aLgorithm Optimizer

AHTR Optimization for Non-Conventional Designs

Conclusion

Overview

Background: Advanced High Temperature Reactor

Objectives: AHTR Model Development

Background: Generative Reactor Design Optimization

Objectives: AHTR Optimization for Non-Conventional Designs

Summary

Advanced High Temperature Reactor Geometry

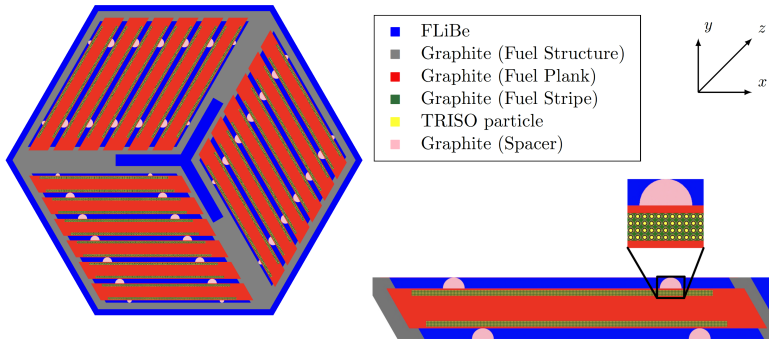


Figure 3: AHTR full assembly with 18 fuel plates arranged in three diamond-shaped sectors, with a central Y-shaped and external channel graphite structure.

The AHTR has **triple heterogeneity**: hexagonal fuel elements within the core, and TRISO particles embedded in stripes within each plank.

Introduction

FHR Benchmark Results

AHTR Temperature Model Verification and Results

ROLLO: Reactor evOLutionary aLgorithm Optimizer

AHTR Optimization for Non-Conventional Designs

Conclusion

Overview

Background: Advanced High Temperature Reactor

Objectives: AHTR Model Development

Background: Generative Reactor Design Optimization

Objectives: AHTR Optimization for Non-Conventional Designs

Summary

FHR Benchmark



The AHTR's geometry's triple heterogeneity results in **complex reactor physics** and **significant modeling challenges**.

- Many surfaces to model = computationally expensive
- Homogenization might result in loss of reactor physics effects

Introduction

FHR Benchmark Results

AHTR Temperature Model Verification and Results

ROLLO: Reactor evOLutionary aLgorithm Optimizer

AHTR Optimization for Non-Conventional Designs

Conclusion

Overview

Background: Advanced High Temperature Reactor

Objectives: AHTR Model Development

Background: Generative Reactor Design Optimization

Objectives: AHTR Optimization for Non-Conventional Designs

Summary

FHR Benchmark



The AHTR's geometry's triple heterogeneity results in **complex reactor physics** and **significant modeling challenges**.

- Many surfaces to model = computationally expensive
- Homogenization might result in loss of reactor physics effects

In 2019 the **OECD-NEA initiated the FHR benchmark**. Its objective is to identify the applicability, accuracy, and practicality of the latest methods and codes to assess the current state of the art for FHR modeling.

The screenshot shows the official website of the Nuclear Energy Agency (NEA). The header includes the NEA logo, "NUCLEAR ENERGY AGENCY", and navigation links for "ABOUT US", "TOPICS", and a menu icon. Below the header is a search bar with a magnifying glass icon. The main content area features a large title "Fluoride Salt-Cooled High-Temperature Reactor (FHR) Benchmark" and a blue "Ongoing" status indicator. At the bottom, there are category tags: "Molten salt reactors", "Nuclear science", "Reactor physics", and an ellipsis.

Fluoride Salt-Cooled High-Temperature Reactor (FHR) Benchmark

Ongoing

Molten salt reactors Nuclear science Reactor physics ...

Introduction

FHR Benchmark Results

AHTR Temperature Model Verification and Results

ROLLO: Reactor evOLutionary aLgorithm Optimizer

AHTR Optimization for Non-Conventional Designs

Conclusion

Overview

Background: Advanced High Temperature Reactor

Objectives: AHTR Model Development

Background: Generative Reactor Design Optimization

Objectives: AHTR Optimization for Non-Conventional Designs

Summary

Research Objectives: AHTR Model Development



Technical Gap

The geometrically complex AHTR design is challenging to model accurately and computationally expensive.

Introduction

FHR Benchmark Results

AHTR Temperature Model Verification and Results

ROLLO: Reactor evOLutionary aLgorithm Optimizer

AHTR Optimization for Non-Conventional Designs

Conclusion

Overview

Background: Advanced High Temperature Reactor

Objectives: AHTR Model Development

Background: Generative Reactor Design Optimization

Objectives: AHTR Optimization for Non-Conventional Designs

Summary

Research Objectives: AHTR Model Development



Technical Gap

The geometrically complex AHTR design is challenging to model accurately and computationally expensive.

Research Objectives: AHTR Model Development

- Participate in FHR benchmark's neutronics modeling to further our understanding of the AHTR design's complexities
- AHTR temperature model to capture thermal feedback effects

Introduction

FHR Benchmark Results

AHTR Temperature Model Verification and Results

ROLLO: Reactor evOLutionary aLgorithm Optimizer

AHTR Optimization for Non-Conventional Designs

Conclusion

Overview

Background: Advanced High Temperature Reactor

Objectives: AHTR Model Development

Background: Generative Reactor Design Optimization

Objectives: AHTR Optimization for Non-Conventional Designs

Summary

Research Objectives: AHTR Model Development



Technical Gap

The geometrically complex AHTR design is challenging to model accurately and computationally expensive.

Research Objectives: AHTR Model Development

- Participate in FHR benchmark's neutronics modeling to further our understanding of the AHTR design's complexities
- AHTR temperature model to capture thermal feedback effects

Link to Reactor Optimization for Non-conventional Designs

- By participating in the benchmark, I ensure an accurate AHTR base model
- Thus, I can expect accurate answers for the optimized AHTR designs

Overview



In this defense, I will show that I successfully:

- ① Furthered our understanding of the AHTR design's complexities through neutronics and temperature modeling
- ② Created an open-source tool that enables reactor generative design optimization with evolutionary algorithms
- ③ Applied the optimization tool to the AHTR design for non-conventional geometries and fuel distributions

Introduction

FHR Benchmark Results

AHTR Temperature Model Verification and Results

ROLLO: Reactor evOLutionary aLgorithm Optimizer

AHTR Optimization for Non-Conventional Designs

Conclusion

Overview

Background: Advanced High Temperature Reactor

Objectives: AHTR Model Development

Background: Generative Reactor Design Optimization

Objectives: AHTR Optimization for Non-Conventional Designs

Summary

3D Printing a Nuclear Reactor



Additive manufacturing enables us to **surpass classical manufacturing constraints** and optimize for **arbitrary geometries and parameters**.

With further advancement of additive manufacturing technologies, a reactor core could be 3D printed within the next decade.

Introduction

FHR Benchmark Results

AHTR Temperature Model Verification and Results

ROLLO: Reactor evOLutionary aLgorithm Optimizer

AHTR Optimization for Non-Conventional Designs

Conclusion

Overview

Background: Advanced High Temperature Reactor

Objectives: AHTR Model Development

Background: Generative Reactor Design Optimization

Objectives: AHTR Optimization for Non-Conventional Designs

Summary

3D Printing a Nuclear Reactor



Additive manufacturing enables us to **surpass classical manufacturing constraints** and optimize for **arbitrary geometries and parameters**.

With further advancement of additive manufacturing technologies, a reactor core could be 3D printed within the next decade.

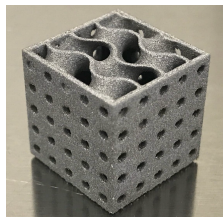


Figure 5: 3D printed Tungsten wavy flow channels, reproduced from NASA's Refractory Alloy Additive Manufacturing Build Optimization Project (RAAMBO) [3].

Introduction

FHR Benchmark Results

AHTR Temperature Model Verification and Results

ROLLO: Reactor evOLutionary aLgorithm Optimizer

AHTR Optimization for Non-Conventional Designs

Conclusion

Overview

Background: Advanced High Temperature Reactor

Objectives: AHTR Model Development

Background: Generative Reactor Design Optimization

Objectives: AHTR Optimization for Non-Conventional Designs

Summary

3D Printing a Nuclear Reactor



Additive manufacturing enables us to **surpass classical manufacturing constraints** and optimize for **arbitrary geometries and parameters**.

With further advancement of additive manufacturing technologies, a reactor core could be 3D printed within the next decade.

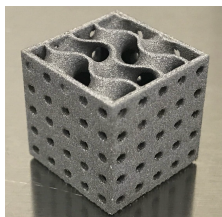


Figure 5: 3D printed Tungsten wavy flow channels, reproduced from NASA's Refractory Alloy Additive Manufacturing Build Optimization Project (RAAMBO) [3].

Wide-spread adoption of 3D printing for reactor parts could **reduce fabrication costs and deployment timelines, and improve reactor safety and performance**.

Introduction

FHR Benchmark Results

AHTR Temperature Model Verification and Results

ROLLO: Reactor evOLutionary aLgorithm Optimizer

AHTR Optimization for Non-Conventional Designs

Conclusion

Overview

Background: Advanced High Temperature Reactor

Objectives: AHTR Model Development

Background: Generative Reactor Design Optimization

Objectives: AHTR Optimization for Non-Conventional Designs

Summary



3D Printing a Nuclear Reactor

Additive manufacturing enables us to **surpass classical manufacturing constraints** and optimize for **arbitrary geometries and parameters**.

With further advancement of additive manufacturing technologies, a reactor core could be 3D printed within the next decade.

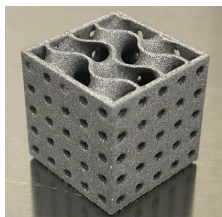


Figure 5: 3D printed Tungsten wavy flow channels, reproduced from NASA's Refractory Alloy Additive Manufacturing Build Optimization Project (RAAMBO) [3].

Wide-spread adoption of 3D printing for reactor parts could **reduce fabrication costs and deployment timelines, and improve reactor safety and performance**.

To explore the new design space enabled by 3D printing more fficiently, we require methods, such as **generative design**.

Introduction

FHR Benchmark Results

AHTR Temperature Model Verification and Results

ROLLO: Reactor evOLutionary aLgorithm Optimizer

AHTR Optimization for Non-Conventional Designs

Conclusion

Overview

Background: Advanced High Temperature Reactor

Objectives: AHTR Model Development

Background: Generative Reactor Design Optimization

Objectives: AHTR Optimization for Non-Conventional Designs

Summary

Generative Reactor Design Optimization



Generative design is an **iterative design exploration process** [4].

- Designers provide design goals and constraints to the generative design software
- Software explores all the possible permutations of a solution, quickly generating design alternatives

Introduction

FHR Benchmark Results

AHTR Temperature Model Verification and Results

ROLLO: Reactor evOLutionary aLgorithm Optimizer

AHTR Optimization for Non-Conventional Designs

Conclusion

Overview

Background: Advanced High Temperature Reactor

Objectives: AHTR Model Development

Background: Generative Reactor Design Optimization

Objectives: AHTR Optimization for Non-Conventional Designs

Summary

Generative Reactor Design Optimization



Generative design is an **iterative design exploration process** [4].

- Designers provide design goals and constraints to the generative design software
- Software explores all the possible permutations of a solution, quickly generating design alternatives

The generative design software **automates the search process for suitable geometries**.

The human reactor designer can instead focus on

- **Defining design criteria** for optimal designs
- **Evaluating the results** generated by generative design software

Introduction

FHR Benchmark Results

AHTR Temperature Model Verification and Results

ROLLO: Reactor evOLutionary aLgorithm Optimizer

AHTR Optimization for Non-Conventional Designs

Conclusion

Overview

Background: Advanced High Temperature Reactor

Objectives: AHTR Model Development

Background: Generative Reactor Design Optimization

Objectives: AHTR Optimization for Non-Conventional Designs

Summary

Generative Reactor Design Optimization



Generative design is an **iterative design exploration process** [4].

- Designers provide design goals and constraints to the generative design software
- Software explores all the possible permutations of a solution, quickly generating design alternatives

The generative design software **automates the search process for suitable geometries**.

The human reactor designer can instead focus on

- **Defining design criteria** for optimal designs
- **Evaluating the results** generated by generative design software

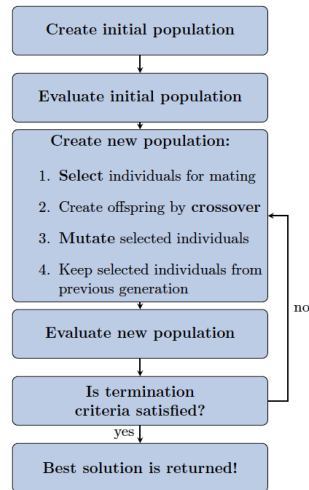
Evolutionary algorithms can be used to **drive generative reactor design optimization** to promptly explore the large design space to find global optimal designs.

Evolutionary Algorithms for Reactor Generative Design



Evolutionary Algorithms

- **Imitate natural selection** to evolve solutions
- Uses simple mechanisms: **selection** (selects good individuals), **mutation** and **crossover** (creates better individuals)
- **Average population improves with every generation**



Evolutionary Algorithms for Reactor Generative Design

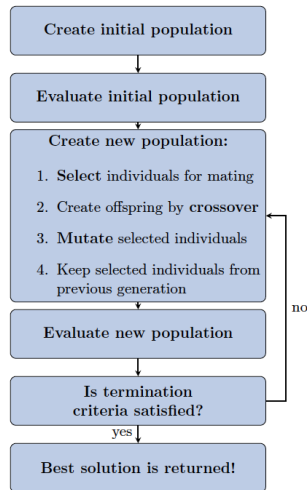


Evolutionary Algorithms

- **Imitate natural selection** to evolve solutions
- Uses simple mechanisms: **selection** (selects good individuals), **mutation** and **crossover** (creates better individuals)
- **Average population improves with every generation**

Evolutionary Algorithm Benefits

- **Computationally simple**
- Proven to be successful at finding **globally optimal solutions** for multi-objective optimization problems
- Can take advantage of **parallel systems**



Introduction

FHR Benchmark Results

AHTR Temperature Model Verification and Results

ROLLO: Reactor evOLutionary aLgorithm Optimizer

AHTR Optimization for Non-Conventional Designs

Conclusion

Overview

Background: Advanced High Temperature Reactor

Objectives: AHTR Model Development

Background: Generative Reactor Design Optimization

Objectives: AHTR Optimization for Non-Conventional Designs

Summary

Research Objectives: AHTR optimization for non-conventional designs

Technical Gap

- Optimization tools for generating new reactor designs enabled by 3D printing do not exist
- Few demonstrations of reactor optimization for non-conventional geometries and parameters exist

Introduction

FHR Benchmark Results

AHTR Temperature Model Verification and Results

ROLLO: Reactor evOLutionary aLgorithm Optimizer

AHTR Optimization for Non-Conventional Designs

Conclusion

Overview

Background: Advanced High Temperature Reactor

Objectives: AHTR Model Development

Background: Generative Reactor Design Optimization

Objectives: AHTR Optimization for Non-Conventional Designs

Summary

Research Objectives: AHTR optimization for non-conventional designs

Technical Gap

- Optimization tools for generating new reactor designs enabled by 3D printing do not exist
- Few demonstrations of reactor optimization for non-conventional geometries and parameters exist

Research Objectives: AHTR optimization for non-conventional designs

- Develop an open-source tool that enables generative reactor design optimization with evolutionary algorithms
- Demonstrate successful tool application on AHTR optimization for non-conventional reactor geometries and fuel distributions

Introduction

FHR Benchmark Results

AHTR Temperature Model Verification and Results

ROLLO: Reactor evOLutionary aLgorithm Optimizer

AHTR Optimization for Non-Conventional Designs

Conclusion

Overview

Background: Advanced High Temperature Reactor

Objectives: AHTR Model Development

Background: Generative Reactor Design Optimization

Objectives: AHTR Optimization for Non-Conventional Designs

Summary

Research Objectives Summary



Research Objectives: AHTR Model Development

- Participate in the OECD-NEA's FHR Benchmark with OpenMC [5]
- AHTR temperature model with Moltres [6]

Introduction

FHR Benchmark Results

AHTR Temperature Model Verification and Results

ROLLO: Reactor evOLutionary aLgorithm Optimizer

AHTR Optimization for Non-Conventional Designs

Conclusion

Overview

Background: Advanced High Temperature Reactor

Objectives: AHTR Model Development

Background: Generative Reactor Design Optimization

Objectives: AHTR Optimization for Non-Conventional Designs

Summary

Research Objectives Summary



Research Objectives: AHTR Model Development

- Participate in the OECD-NEA's FHR Benchmark with OpenMC [5]
- AHTR temperature model with Moltres [6]

Research Objectives: AHTR optimization for non-conventional designs

- Develop an open-source tool that enables generative reactor design optimization with evolutionary algorithms
- Demonstrate successful tool application on AHTR optimization for non-conventional reactor geometries and fuel distributions

Outline

① Introduction

Overview

Background: Advanced High Temperature Reactor

Objectives: AHTR Model Development

Background: Generative Reactor Design Optimization

Objectives: AHTR Optimization for Non-Conventional Designs

Summary

② FHR Benchmark Results

FHR Benchmark Specifications

FHR Benchmark Results

③ AHTR Temperature Model Verification and Results

AHTR Temperature Model with Moltres

Key Neutronics Parameters Verification

AHTR Temperature Model Results

Summary

④ ROLLO: Reactor evOLutionary aLgorithm Optimizer

ROLLO: Reactor evOLutionary aLgorithm Optimizer

⑤ AHTR Optimization for Non-Conventional Designs

Optimization Methodology

AHTR One-Third Assembly Optimization Results

⑥ Conclusion

Conclusion

Future Work

FHR Benchmark Specifications



The UIUC team participates in the FHR benchmark with the **OpenMC** [5] code and the **ENDF/B-VII.1 material cross-section library** [7].

The OpenMC Code

- Continuous-energy Monte Carlo neutron transport code
- Open-source and hosted on Github

FHR Benchmark Specifications



The UIUC team participates in the FHR benchmark with the **OpenMC** [5] code and the **ENDF/B-VII.1 material cross-section library** [7].

The OpenMC Code

- Continuous-energy Monte Carlo neutron transport code
- Open-source and hosted on Github

FHR Benchmark Completed Phases:

- **Phase I-A:** 2D full assembly steady state model
- **Phase I-B:** 2D full assembly depletion model

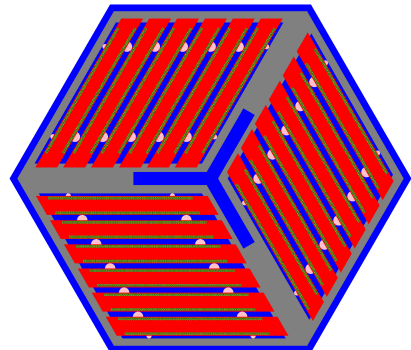


Figure 6: AHTR full assembly.

FHR Benchmark Phase I-A Results



Table 1: FHR Benchmark Phase I-A (2D assembly steady state model) results [8].

Case	Summary	k_{eff}^*	Fuel $\frac{\Delta\rho}{\Delta T}$	FliBe $\frac{\Delta\rho}{\Delta T}$	Graphite $\frac{\Delta\rho}{\Delta T}$
1A	<ul style="list-style-type: none"> Reference case • 9 wt% enrichment • Hot full power • no BP and CR 	1.39389	-2.24±0.15	-0.15±0.15	-0.68±0.15
2AH	<ul style="list-style-type: none"> Hot zero power 	1.40395	-3.14±0.15	-0.20±0.14	-0.85±0.14
2AC	<ul style="list-style-type: none"> Cold zero power 	1.41891	-3.36±0.14	-0.11±0.14	0.07±0.14
3A	<ul style="list-style-type: none"> Control rod inserted 	1.03147	-4.03±0.28	-0.83±0.27	-3.18±0.29
4A	<ul style="list-style-type: none"> Discrete burnable poison 	1.09766	-4.06±0.24	-1.55±0.23	-6.51±0.24
4AR	<ul style="list-style-type: none"> Discrete BP • CR inserted 	0.84158	-5.60±0.49	-1.78±0.46	-10.44±0.47
5A	<ul style="list-style-type: none"> Dispersed burnable poison 	0.79837	-5.09±0.40	-4.87±0.40	-22.99±0.38
6A	<ul style="list-style-type: none"> Double TRISO particle fuel 	1.26294	-4.46±0.19	0.16±0.20	-0.39±0.20
7A	<ul style="list-style-type: none"> 19.75 wt% enrichment 	1.50526	-2.49±0.13	-0.12±0.12	-0.62±0.12

BP: burnable poison, CR: control rod

* All k_{eff} values have an uncertainty of 0.00010.

500 active cycles, 100 inactive cycles, and 200000 neutrons UIUC's BlueWaters supercomputer with 64 XE nodes



FHR Benchmark Phase I-A Results

k_{eff} : **Effective neutron multiplication factor**, average number of neutrons from one fission that cause another fission.

Case	Summary	k_{eff}^*	Fuel $\frac{\Delta\rho}{\Delta T}$	FliBe $\frac{\Delta\rho}{\Delta T}$	Graphite $\frac{\Delta\rho}{\Delta T}$
1A	<ul style="list-style-type: none"> Reference case • 9 wt% enrichment • Hot full power • no BP and CR 	1.39389	-2.24±0.15	-0.15±0.15	-0.68±0.15
2AH	• Hot zero power	1.40395	-3.14±0.15	-0.20±0.14	-0.85±0.14
2AC	• Cold zero power	1.41891	-3.36±0.14	-0.11±0.14	0.07±0.14
3A	• Control rod inserted	1.03147	-4.03±0.28	-0.83±0.27	-3.18±0.29
4A	• Discrete burnable poison	1.09766	-4.06±0.24	-1.55±0.23	-6.51±0.24
4AR	• Discrete BP • CR inserted	0.84158	-5.60±0.49	-1.78±0.46	-10.44±0.47
5A	• Dispersed burnable poison	0.79837	-5.09±0.40	-4.87±0.40	-22.99±0.38
6A	• Double TRISO particle fuel	1.26294	-4.46±0.19	0.16±0.20	-0.39±0.20
7A	• 19.75 wt% enrichment	1.50526	-2.49±0.13	-0.12±0.12	-0.62±0.12

BP: burnable poison, CR: control rod

* All k_{eff} values have an uncertainty of 0.00010.

Increased fuel packing does not always correspond with increased k_{eff} due to spatial self-shielding effects.



FHR Benchmark Phase I-A Results

Reactivity coefficients: how much k_{eff} is changing when temperature of the material changes.

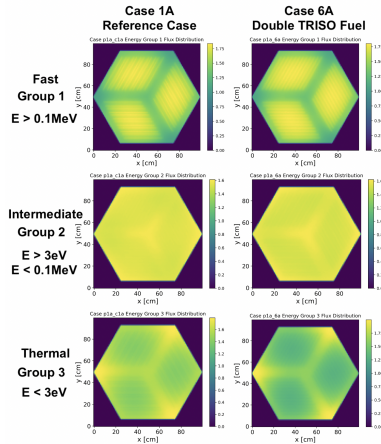
Case	Summary	k_{eff}^*	Fuel $\frac{\Delta\rho}{\Delta T}$	FliBe $\frac{\Delta\rho}{\Delta T}$	Graphite $\frac{\Delta\rho}{\Delta T}$
1A	<ul style="list-style-type: none"> Reference case • 9 wt% enrichment • Hot full power • no BP and CR 	1.39389	-2.24±0.15	-0.15±0.15	-0.68±0.15
2AH	<ul style="list-style-type: none"> Hot zero power 	1.40395	-3.14±0.15	-0.20±0.14	-0.85±0.14
2AC	<ul style="list-style-type: none"> Cold zero power 	1.41891	-3.36±0.14	-0.11±0.14	0.07±0.14
3A	<ul style="list-style-type: none"> Control rod inserted 	1.03147	-4.03±0.28	-0.83±0.27	-3.18±0.29
4A	<ul style="list-style-type: none"> Discrete burnable poison 	1.09766	-4.06±0.24	-1.55±0.23	-6.51±0.24
4AR	<ul style="list-style-type: none"> Discrete BP • CR inserted 	0.84158	-5.60±0.49	-1.78±0.46	-10.44±0.47
5A	<ul style="list-style-type: none"> Dispersed burnable poison 	0.79837	-5.09±0.40	-4.87±0.40	-22.99±0.38
6A	<ul style="list-style-type: none"> Double TRISO particle fuel 	1.26294	-4.46±0.19	0.16±0.20	-0.39±0.20
7A	<ul style="list-style-type: none"> 19.75 wt% enrichment 	1.50526	-2.49±0.13	-0.12±0.12	-0.62±0.12

BP: burnable poison, CR: control rod

* All k_{eff} values have an uncertainty of 0.00010.

Most of the temperature coefficients are negative, exemplifying the AHTR's passive safety behavior.

FHR Benchmark Phase I-A Results

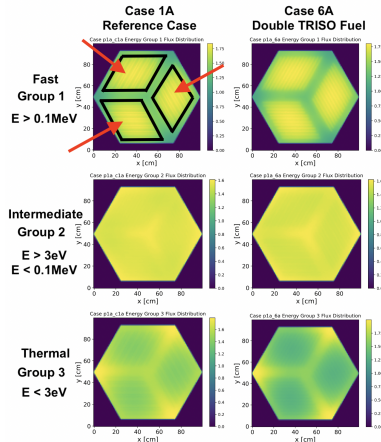


Key Takeaways



Figure 7: Neutron flux distribution.

FHR Benchmark Phase I-A Results

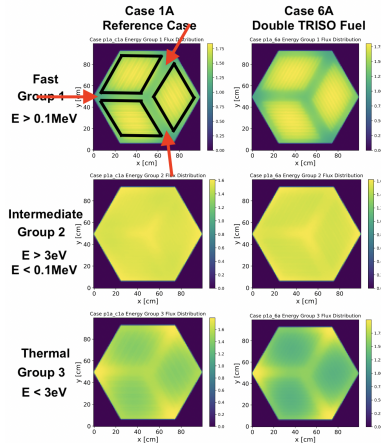


Key Takeaways

- Peak in Group 1 fast neutrons born in assembly diamond's center

Figure 7: Neutron flux distribution.

FHR Benchmark Phase I-A Results



Key Takeaways

- Peak in Group 1 fast neutrons born in assembly diamond's center
- Fast neutrons are moderated in graphite matrix and structure

Figure 7: Neutron flux distribution.

FHR Benchmark Phase I-A Results

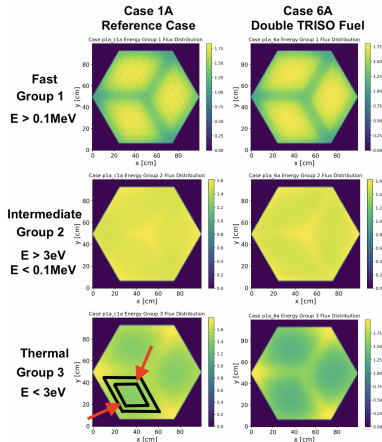


Figure 7: Neutron flux distribution.

Key Takeaways

- Peak in Group 1 fast neutrons born in assembly diamond's center
- Fast neutrons are moderated in graphite matrix and structure
- Outer diamond's sides absorb the moderated thermal neutrons and **geometrically shield the assembly diamond's center from neutron thermal flux**

FHR Benchmark Phase I-A Results

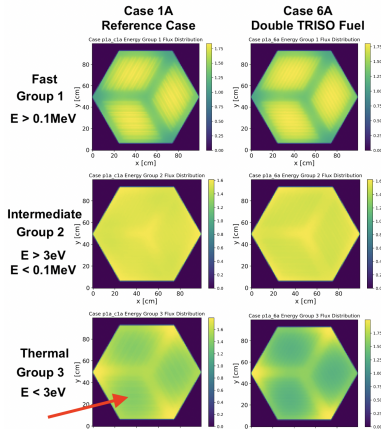


Figure 7: Neutron flux distribution.

Key Takeaways

- Peak in Group 1 fast neutrons born in assembly diamond's center
- Fast neutrons are moderated in graphite matrix and structure
- Outer diamond's sides absorb the moderated thermal neutrons and **geometrically shield the assembly diamond's center from neutron thermal flux**
- Results in a dip in thermal Group 3 flux in the assembly diamond's center

FHR Benchmark Phase I-A Results

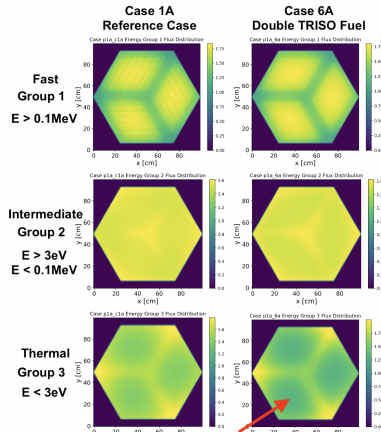


Figure 7: Neutron flux distribution.

Key Takeaways

- Peak in Group 1 fast neutrons born in assembly diamond's center
- Fast neutrons are moderated in graphite matrix and structure
- Outer diamond's sides absorb the moderated thermal neutrons and **geometrically shield the assembly diamond's center from neutron thermal flux**
- Results in a dip in thermal Group 3 flux in the assembly diamond's center
- This self-shielding effect is more pronounced in Case 6A**

FHR Benchmark Phase I-A Results



In an ANS M&C 2021 conference paper we compared FHR benchmark participants' Phase I-A results.

ANS M&C 2021 - The International Conference on Mathematics and Computational Methods Applied to Nuclear Science and Engineering · Raleigh, North Carolina · October 3–7, 2021

PRELIMINARY RESULTS OF THE NEA FHR BENCHMARK PHASE I-A AND I-B (FUEL ELEMENT 2-D BENCHMARK)

B. Petrovic^{1*}, K. Ramey¹, I. Hill², E. Lossa³, M. Elsawi⁴, Z. Wu⁵, C. Lu⁵, J. Gonzalez⁶, D. Novog⁶, G. Chee⁷, K. Huff⁷, M. Margulis⁸, N. Read⁸ and E. Shwageraus⁸

[Figure 8: FHR benchmark paper presented at M&C 2021 \[9\].](#)

FHR Benchmark Phase I-A Results



In an ANS M&C 2021 conference paper we compared FHR benchmark participants' Phase I-A results.

ANS M&C 2021 - The International Conference on Mathematics and Computational Methods Applied to Nuclear Science and Engineering · Raleigh, North Carolina · October 3–7, 2021

PRELIMINARY RESULTS OF THE NEA FHR BENCHMARK PHASE I-A AND I-B (FUEL ELEMENT 2-D BENCHMARK)

B. Petrovic^{1*}, K. Ramey¹, I. Hill², E. Losa³, M. Elsawi⁴, Z. Wu⁵, C. Lu⁵, J. Gonzalez⁶, D. Novog⁶, G. Chee⁷, K. Huff⁷, M. Margulis⁸, N. Read⁸ and E. Shwageraus⁸

Figure 8: FHR benchmark paper presented at M&C 2021 [9].

The k_{eff} standard deviation between participants for each case was in the 231 to 514 pcm range, **acceptable and notably close** given a blind benchmark.

FHR Benchmark Phase I-A Results



In an ANS M&C 2021 conference paper we compared FHR benchmark participants' Phase I-A results.

ANS M&C 2021 - The International Conference on Mathematics and Computational Methods Applied to Nuclear Science and Engineering · Raleigh, North Carolina · October 3–7, 2021

PRELIMINARY RESULTS OF THE NEA FHR BENCHMARK PHASE I-A AND I-B (FUEL ELEMENT 2-D BENCHMARK)

B. Petrovic^{1*}, K. Ramey¹, I. Hill², E. Losa³, M. Elsawi⁴, Z. Wu⁵, C. Lu⁵, J. Gonzalez⁶, D. Novog⁶, G. Chee⁷, K. Huff⁷, M. Margulis⁸, N. Read⁸ and E. Shwageraus⁸

[Figure 8: FHR benchmark paper presented at M&C 2021 \[9\].](#)

The k_{eff} standard deviation between participants for each case was in the 231 to 514 pcm range, **acceptable and notably close** given a blind benchmark.

This gives **confidence to the AHTR base model's accuracy**, as I proceed to optimize the AHTR for non-conventional geometries.

Outline

1 Introduction

Overview

Background: Advanced High Temperature Reactor

Objectives: AHTR Model Development

Background: Generative Reactor Design Optimization

Objectives: AHTR Optimization for Non-Conventional Designs

Summary

2 FHR Benchmark Results

FHR Benchmark Specifications

FHR Benchmark Results

3 AHTR Temperature Model Verification and Results

AHTR Temperature Model with Moltres

Key Neutronics Parameters Verification

AHTR Temperature Model Results

Summary

4 ROLLO: Reactor evOLutionary aLgorithm Optimizer

ROLLO: Reactor evOLutionary aLgorithm Optimizer

5 AHTR Optimization for Non-Conventional Designs

Optimization Methodology

AHTR One-Third Assembly Optimization Results

6 Conclusion

Conclusion

Future Work

AHTR Temperature Model

An **AHTR temperature model** captures **thermal feedback effects**, absent from the purely neutronics FHR Benchmark simulations.



AHTR Temperature Model



An **AHTR temperature model** captures **thermal feedback effects**, absent from the purely neutronics FHR Benchmark simulations.

Moltres [6]

- An application built on the Multiphysics Object-Oriented Simulation Environment (MOOSE) framework, for the simulation of MSRs
- MOOSE [10] is an open source finite element framework written in C++ that relies on Libmesh and PETSc for meshing and PDE solving capabilities
- Moltres can run transient, implicitly coupled neutronics/thermal-hydraulics simulations
 - Multi-group neutron diffusion (arbitrary no. of groups)
 - Delayed neutron precursor decay (with advection)
 - Incompressible Navier-Stokes for temperature advection-diffusion

AHTR Temperature Model



An **AHTR temperature model** captures **thermal feedback effects**, absent from the purely neutronics FHR Benchmark simulations.

Moltres [6]

- An application built on the Multiphysics Object-Oriented Simulation Environment (MOOSE) framework, for the simulation of MSRs
- MOOSE [10] is an open source finite element framework written in C++ that relies on Libmesh and PETSc for meshing and PDE solving capabilities
- Moltres can run transient, implicitly coupled neutronics/thermal-hydraulics simulations
 - Multi-group neutron diffusion (arbitrary no. of groups)
 - Delayed neutron precursor decay (with advection)
 - Incompressible Navier-Stokes for temperature advection-diffusion

AHTR Temperature Model with Moltres

- I model the AHTR full assembly's 2D XY steady-state temperature
- Assumptions: conductive heat transfer, heat removal by uniform salt flow in coolant regions

AHTR Temperature Model Setup



Steps to produce Moltres AHTR Temperature Model

- OpenMC neutronics model produces **group constants cross-section data** (various macroscopic neutron cross sections, neutron diffusion coefficient, etc.)
- **Mesh generation** with Gmsh [11]
- **Run Moltres model:** using these group constants and mesh, Moltres solves for the flux and temperature based on the neutron diffusion equation coupled with temperature advection due to coolant flow

AHTR Temperature Model Setup



Steps to produce Moltres AHTR Temperature Model

- OpenMC neutronics model produces **group constants cross-section data** (various macroscopic neutron cross sections, neutron diffusion coefficient, etc.)
- **Mesh generation** with Gmsh [11]
- **Run Moltres model:** using these group constants and mesh, Moltres solves for the flux and temperature based on the neutron diffusion equation coupled with temperature advection due to coolant flow

Unlike the OpenMC neutronics model, **Moltres does not explicitly model each TRISO particle** because a TRISO-level fidelity mesh file is impractical and will result in an extremely long Moltres runtimes.

AHTR Temperature Model Setup



Steps to produce Moltres AHTR Temperature Model

- OpenMC neutronics model produces **group constants cross-section data** (various macroscopic neutron cross sections, neutron diffusion coefficient, etc.)
- **Mesh generation** with Gmsh [11]
- **Run Moltres model:** using these group constants and mesh, Moltres solves for the flux and temperature based on the neutron diffusion equation coupled with temperature advection due to coolant flow

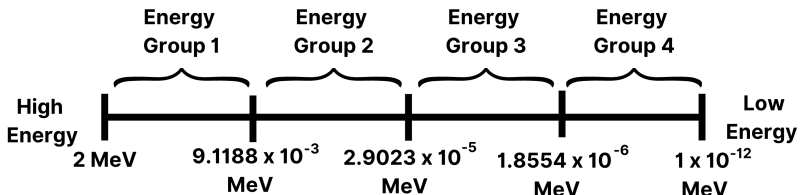
Unlike the OpenMC neutronics model, **Moltres does not explicitly model each TRISO particle** because a TRISO-level fidelity mesh file is impractical and will result in an extremely long Moltres runtimes.

For successful AHTR temperature model with Moltres, I must establish **suitable spatial and energy homogenization** to create group constants and mesh that preserve accuracy while maintaining an acceptable runtime.

AHTR Temperature Model Energy Homogenization



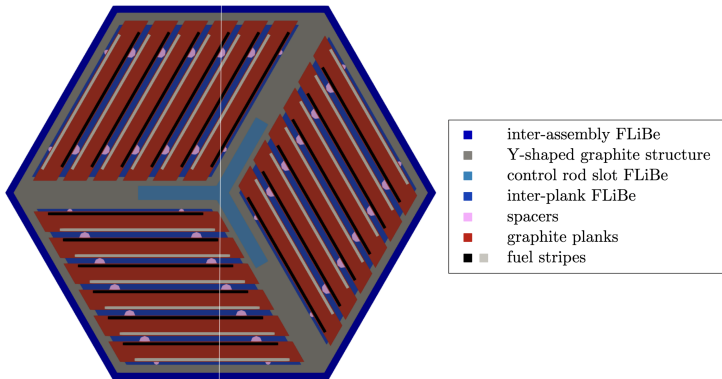
Figure 9: 4-group energy structure used for AHTR modeling derived by Gentry et al [12].
Figure is not to scale.



AHTR Temperature Model Spatial Homogenization



Full assembly 61 cell discretization: inter-assembly FLiBe, Y-shaped graphite structure, control rod slot FLiBe, graphite spacers, each diamond shape section's inter-plank FLiBe (3), each graphite plank (18), and each fuel stripe (36)



AHTR Temp Model Key Neutronics Parameter Verification



I verify acceptable spatial homogenization and energy discretization by comparing key neutronics parameters between:

- OpenMC simulation with continuous energy and TRISO-level spatial fidelity
- Moltres simulation with 4-group energy and spatial homogenization

AHTR Temp Model Key Neutronics Parameter Verification



I verify acceptable spatial homogenization and energy discretization by comparing key neutronics parameters between:

- OpenMC simulation with continuous energy and TRISO-level spatial fidelity
- Moltres simulation with 4-group energy and spatial homogenization

Key Neutronics Parameters: k_{eff} , reactivity coefficients, flux distribution, and neutron energy spectrum

- All comparisons are to verify that the Moltres model is replicating the OpenMC model's neutronics correctly

AHTR Temp Model Key Neutronics Parameter Verification



I verify acceptable spatial homogenization and energy discretization by comparing key neutronics parameters between:

- OpenMC simulation with continuous energy and TRISO-level spatial fidelity
- Moltres simulation with 4-group energy and spatial homogenization

Key Neutronics Parameters: k_{eff} , reactivity coefficients, flux distribution, and neutron energy spectrum

- All comparisons are to verify that the Moltres model is replicating the OpenMC model's neutronics correctly

Reactivity coefficients and flux distribution

- Ensure that Moltres accurately calculates the AHTR's temperature distribution
- Reactivity coefficients capture temperature reactivity feedback on the flux
- Moltres source term is dependent on flux

Key Neutronics Parameter Verification Summary



OpenMC vs Moltres models key observations

- 216 pcm reactivity difference
- Good agreement in reactivity coefficients and 4-group neutron spectrum
- Good agreement in overall flux but larger flux diffs at specific points

Key Neutronics Parameter Verification Summary



OpenMC vs Moltres models key observations

- 216 pcm reactivity difference
- Good agreement in reactivity coefficients and 4-group neutron spectrum
- Good agreement in overall flux but larger flux diffs at specific points

Explanations:

- Reactivity and flux differences due to Moltres' **neutron diffusion method**
- Differences in reactivity and flux at specific points might result in **slightly inaccurate temperatures at certain points**
- Since the reactivity coefficients and overall flux distribution are in agreement, this spatial homogenization and energy discretization are **sufficiently accurate** to calculate and gain an **overall perspective** of the AHTR's temperature distribution

Key Neutronics Parameter Verification Summary



OpenMC vs Moltres models key observations

- 216 pcm reactivity difference
- Good agreement in reactivity coefficients and 4-group neutron spectrum
- Good agreement in overall flux but larger flux diffs at specific points

Explanations:

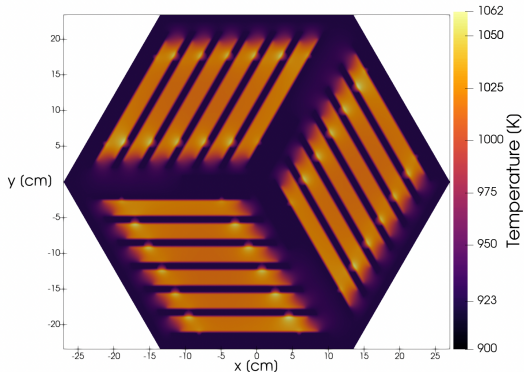
- Reactivity and flux differences due to Moltres' **neutron diffusion method**
- Differences in reactivity and flux at specific points might result in **slightly inaccurate temperatures at certain points**
- Since the reactivity coefficients and overall flux distribution are in agreement, this spatial homogenization and energy discretization are **sufficiently accurate** to calculate and gain an **overall perspective** of the AHTR's temperature distribution

Methodology

- I use this same Moltres model verification method for the AHTR geometries used for optimization



AHTR Temperature Model Results



Results

- Average temperature distribution across the fuel planks are $\approx 1025K$
- Average temperature of graphite structure is $\approx 935K$

Figure 10: 2D temperature distribution in the Advanced High-Temperature Reactor (AHTR) full assembly generated by Moltres.



AHTR Temperature Model Results

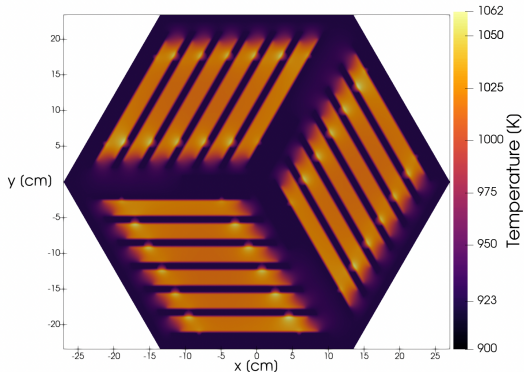


Figure 10: 2D temperature distribution in the Advanced High-Temperature Reactor (AHTR) full assembly generated by Moltres.

Results

- Average temperature distribution across the fuel planks are $\approx 1025\text{K}$
- Average temperature of graphite structure is $\approx 935\text{K}$
- Temperature peaks at 1062K in the fuel stripes near the spacers
- **Temperature peaks are due to the spacers displacing coolant and providing extra moderation**

FHR Benchmark + AHTR Temperature Model: Summary



I Successfully Completed AHTR Model Development Research Objectives

- I participated in the OECD-NEA's FHR Benchmark Phases I-A and I-B
- I modeled the AHTR's temperature distribution with Moltres

FHR Benchmark + AHTR Temperature Model: Summary



I Successfully Completed AHTR Model Development Research Objectives

- I participated in the OECD-NEA's FHR Benchmark Phases I-A and I-B
- I modeled the AHTR's temperature distribution with Moltres

Major Takeaways

- AHTR has passive safety behavior with negative temperature coefficients
- Increased fuel packing does not always correspond with increased k_{eff} due to self-shielding effects
- These results hint at the possibility of **minimizing fuel required by optimizing for heterogenous fuel distributions** within the core
- AHTR temperature peaks in the fuel stripes near the spacers

Outline



① Introduction

- Overview
- Background: Advanced High Temperature Reactor
- Objectives: AHTR Model Development
- Background: Generative Reactor Design Optimization
- Objectives: AHTR Optimization for Non-Conventional Designs
- Summary

② FHR Benchmark Results

- FHR Benchmark Specifications
- FHR Benchmark Results

③ AHTR Temperature Model Verification and Results

- AHTR Temperature Model with Moltres
- Key Neutronics Parameters Verification
- AHTR Temperature Model Results
- Summary

④ ROLLO: Reactor evOLutionary aLgorithm Optimizer

- ROLLO: Reactor evOLutionary aLgorithm Optimizer

⑤ AHTR Optimization for Non-Conventional Designs

- Optimization Methodology
- AHTR One-Third Assembly Optimization Results

⑥ Conclusion

- Conclusion
- Future Work

Research Objectives: AHTR optimization for non-conventional designs

Technical Gap

- Optimization tools for generating new reactor designs enabled by 3D printing do not exist
- Few demonstrations of reactor optimization for non-conventional geometries and parameters exist

Research Objectives: AHTR optimization for non-conventional designs

- Develop an open-source tool that enables generative reactor design optimization with evolutionary algorithms
- Demonstrate successful tool application on AHTR optimization for non-conventional reactor geometries and fuel distributions

ROLLO: Reactor evOLutionary aLgorithm Optimizer



Figure 11: ROLLO (Reactor evOLutionary aLgorithm Optimizer) logo.

- ROLLO (Reactor evOLutionary aLgorithm Optimizer) is a Python package that applies evolutionary algorithms to optimize nuclear reactor design

ROLLO: Reactor evOLutionary aLgorithm Optimizer



Figure 11: ROLLO (Reactor evOLutionary aLgorithm Optimizer) logo.

- ROLLO (Reactor evOLutionary aLgorithm Optimizer) is a Python package that applies evolutionary algorithms to optimize nuclear reactor design
- ROLLO provides a general genetic algorithm framework, sets up parallelization for the user, and promotes usability with an input file that only exposes mandatory parameters

ROLLO: Reactor evOLutionary aLgorithm Optimizer



Figure 11: ROLLO (Reactor evOLutionary aLgorithm Optimizer) logo.

- ROLLO (Reactor evOLutionary aLgorithm Optimizer) is a Python package that applies evolutionary algorithms to optimize nuclear reactor design
- ROLLO provides a general genetic algorithm framework, sets up parallelization for the user, and promotes usability with an input file that only exposes mandatory parameters
- Designed to be: effective, flexible, open-source, parallel, reproducible

How does ROLLO work?

ROLLO Flow

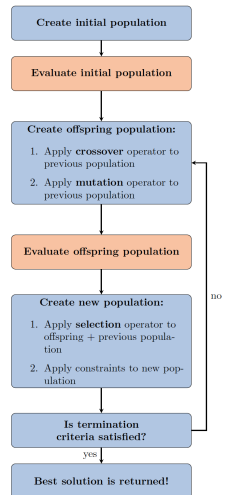
- Reads and validates the JSON input file



How does ROLLO work?

ROLLO Flow

- Reads and validates the JSON input file
- Blue blocks
 - Evolutionary algorithm is driven by Distributed Evolutionary Algorithms in Python (DEAP)
- Orange blocks
 - Reactor modeling software evaluates the fitness of each reactor model in each generation

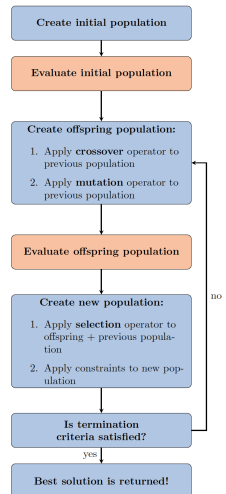


How does ROLLO work?

ROLLO Flow

- Reads and validates the JSON input file
- Blue blocks
 - Evolutionary algorithm is driven by Distributed Evolutionary Algorithms in Python (DEAP)
- Orange blocks
 - Reactor modeling software evaluates the fitness of each reactor model in each generation

For each ROLLO optimization simulation, one must **balance convergence and computational cost.**



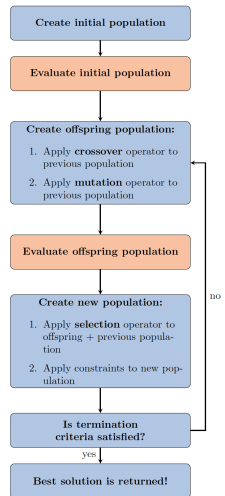
How does ROLLO work?

ROLLO Flow

- Reads and validates the JSON input file
- Blue blocks
 - Evolutionary algorithm is driven by Distributed Evolutionary Algorithms in Python (DEAP)
- Orange blocks
 - Reactor modeling software evaluates the fitness of each reactor model in each generation

For each ROLLO optimization simulation, one must **balance convergence and computational cost**.

ROLLO's purpose is to help the human reactor designer narrow down reactor design search space. The reactor designer uses the **computational power available**, to **narrow down the search space** as much as possible.



Outline

1 Introduction

Overview

Background: Advanced High Temperature Reactor

Objectives: AHTR Model Development

Background: Generative Reactor Design Optimization

Objectives: AHTR Optimization for Non-Conventional Designs

Summary

2 FHR Benchmark Results

FHR Benchmark Specifications

FHR Benchmark Results

3 AHTR Temperature Model Verification and Results

AHTR Temperature Model with Moltres

Key Neutronics Parameters Verification

AHTR Temperature Model Results

Summary

4 ROLLO: Reactor evOLutionary aLgorithm Optimizer

ROLLO: Reactor evOLutionary aLgorithm Optimizer

5 AHTR Optimization for Non-Conventional Designs

Optimization Methodology

AHTR One-Third Assembly Optimization Results

6 Conclusion

Conclusion

Future Work

AHTR Optimization Problem Definitions



Varied Input Parameters

- Total fuel packing fraction (PF_{total})
- TRISO fuel packing fraction distribution ($\rho_{TRISO}(\vec{r})$)
- Coolant channel shape (r_i)

AHTR Optimization Problem Definitions



Varied Input Parameters

- Total fuel packing fraction (PF_{total})
- TRISO fuel packing fraction distribution ($\rho_{TRISO}(\vec{r})$)
- Coolant channel shape (r_i)

Varying PF_{total} and $\rho_{TRISO}(\vec{r})$ synergistically explores how **heterogenous TRISO distribution could minimize self-shielding** and thus, reduce the fuel required.



AHTR Optimization Problem Definitions

Varied Input Parameters

- Total fuel packing fraction (PF_{total})
- TRISO fuel packing fraction distribution ($\rho_{TRISO}(\vec{r})$)
- Coolant channel shape (r_i)

Varying PF_{total} and $\rho_{TRISO}(\vec{r})$ synergistically explores how **heterogenous TRISO distribution could minimize self-shielding** and thus, reduce the fuel required.

AHTR Optimization Objectives

Minimize total fuel packing fraction (PF_{total})

- Cost savings, non-proliferation

Minimize maximum temperature (T_{max})

- Minimize thermal stress in the fuel

Minimize fuel-normalized power peaking factor (PPF_{fuel})

- Efficient fuel utilization

AHTR Optimization Problem Definitions



Varied Input Parameters

- Total fuel packing fraction (PF_{total})
- TRISO fuel packing fraction distribution ($\rho_{TRISO}(\vec{r})$)
- Coolant channel shape (r_i)

Varying PF_{total} and $\rho_{TRISO}(\vec{r})$ synergistically explores how **heterogenous TRISO distribution could minimize self-shielding** and thus, reduce the fuel required.

AHTR Optimization Objectives

Minimize total fuel packing fraction (PF_{total})

- Cost savings, non-proliferation

Minimize maximum temperature (T_{max})

- Minimize thermal stress in the fuel

Minimize fuel-normalized power peaking factor (PPF_{fuel})

- Efficient fuel utilization

I optimized the AHTR plank and one-third assembly geometries.

Introduction

FHR Benchmark Results

AHTR Temperature Model Verification and Results

ROLLO: Reactor evOLutionary aLgorithm Optimizer

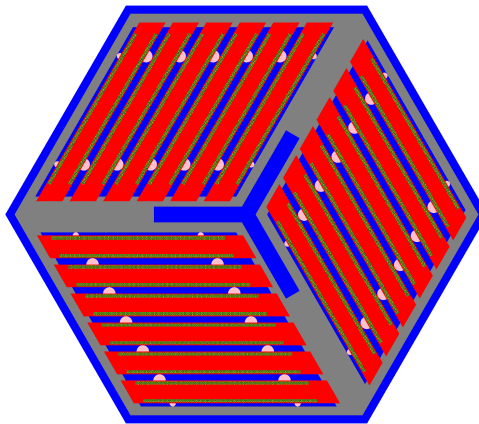
AHTR Optimization for Non-Conventional Designs

Conclusion

Optimization Methodology

AHTR One-Third Assembly Optimization Results

AHTR One-Third Assembly Geometry



Introduction

FHR Benchmark Results

AHTR Temperature Model Verification and Results

ROLLO: Reactor evOLutionary aLgorithm Optimizer

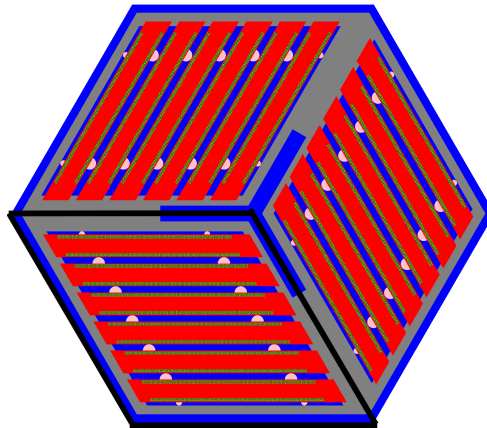
AHTR Optimization for Non-Conventional Designs

Conclusion

Optimization Methodology

AHTR One-Third Assembly Optimization Results

AHTR One-Third Assembly Geometry



AHTR One-Third Assembly Geometry



Two sine distributions govern TRISO packing fraction distribution:

$$\rho_{TRISO}(\vec{x}, \vec{y}) = (\mathbf{a} \cdot \sin(\mathbf{b} \cdot x + \mathbf{c}) + 2) \cdot (\mathbf{d} \cdot \sin(\mathbf{e} \cdot y + \mathbf{f}) + 2) \cdot NF$$

The normalization factor (NF) ensures that total amount of TRISO particles in the one-third assembly corresponds to PF_{total} .

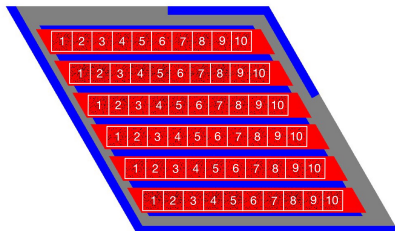


Figure 12: AHTR one-third assembly illustrating packing fraction discretization.



AHTR One-Third Assembly Geometry

Two sine distributions govern TRISO packing fraction distribution:

$$\rho_{TRISO}(\vec{x}, \vec{y}) = (\mathbf{a} \cdot \sin(\mathbf{b} \cdot x + \mathbf{c}) + 2) \cdot (\mathbf{d} \cdot \sin(\mathbf{e} \cdot y + \mathbf{f}) + 2) \cdot NF$$

The normalization factor (NF) ensures that total amount of TRISO particles in the one-third assembly corresponds to PF_{total} .

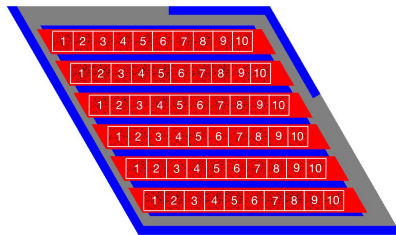


Figure 12: AHTR one-third assembly illustrating packing fraction discretization.

$$\begin{aligned} \mathbf{a} &= 1.435, \mathbf{b} = 1.488, \mathbf{c} = 2.362, \\ \mathbf{d} &= 0.689, \mathbf{e} = 0.584, \mathbf{f} = 4.170 \end{aligned}$$

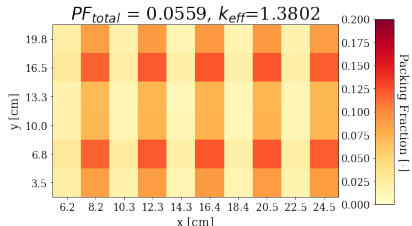


Figure 13: TRISO distribution example.



AHTR One-Third Assembly Geometry

Two sine distributions govern TRISO packing fraction distribution:

$$\rho_{TRISO}(\vec{x}, \vec{y}) = (\mathbf{a} \cdot \sin(\mathbf{b} \cdot x + \mathbf{c}) + 2) \cdot (\mathbf{d} \cdot \sin(\mathbf{e} \cdot y + \mathbf{f}) + 2) \cdot NF$$

The normalization factor (NF) ensures that total amount of TRISO particles in the one-third assembly corresponds to PF_{total} .

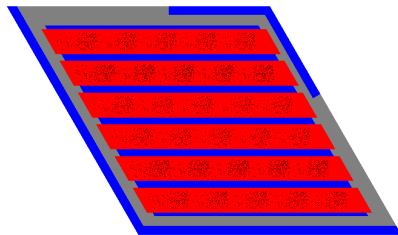


Figure 12: AHTR one-third assembly illustrating packing fraction variation.

$$\mathbf{a} = 1.435, \mathbf{b} = 1.488, \mathbf{c} = 2.362, \\ \mathbf{d} = 0.689, \mathbf{e} = 0.584, \mathbf{f} = 4.170$$

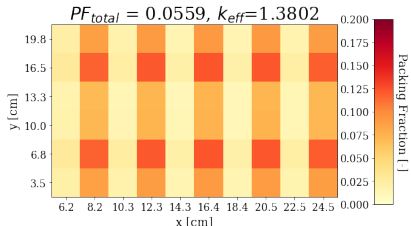


Figure 13: TRISO distribution example.



Contd. AHTR One-Third Assembly Geometry

Five radius values (r_1, r_2, r_3, r_4, r_5) control coolant channel shape.

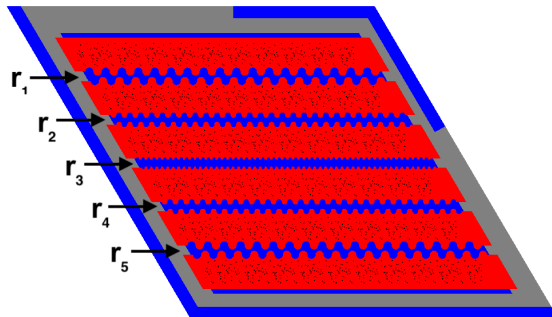
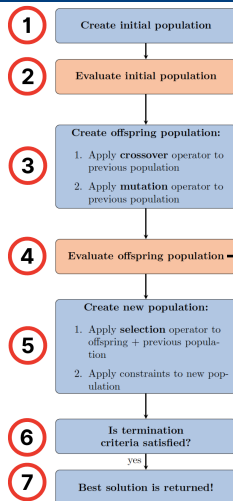


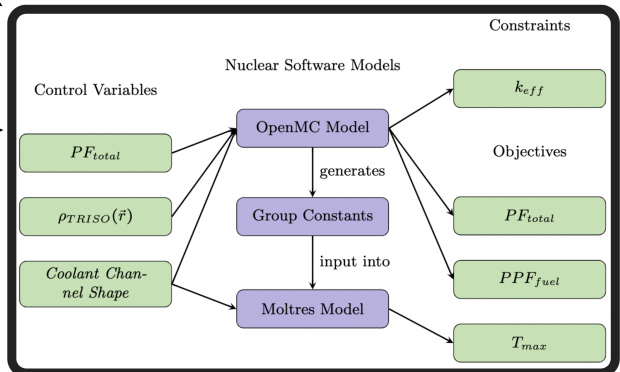
Figure 14: AHTR one-third assembly with coolant channel shape variation,
 $r_1, r_2, r_3, r_4, r_5 = 0.3\text{cm}, 0.2\text{cm}, 0.1\text{cm}, 0.2\text{cm}, 0.3\text{cm}$.

ROLLO AHTR Optimization Workflow



ROLLO Genetic Algorithm Flow

2 4 One AHTR Modeling Workflow



AHTR One-Third Assembly Optimization Simulations

Objs [#]	Sim	Objectives	Constraints	Varying Parameters	Total Compute Cost [node-hours]
1	a-1a	<ul style="list-style-type: none"> • $\min(PF_{total})$ 	<ul style="list-style-type: none"> • $k_{eff} \geq 1.38$ 	<ul style="list-style-type: none"> • $\rho_{TRISO}(\vec{r})$ • PF_{total} 	285.8
	a-1b	<ul style="list-style-type: none"> • $\min(T_{max})$ 	<ul style="list-style-type: none"> • $k_{eff} \geq 1.38$ 	<ul style="list-style-type: none"> • $\rho_{TRISO}(\vec{r})$ 	740.9
	a-1c	<ul style="list-style-type: none"> • $\min(PPF_{fuel})$ 	<ul style="list-style-type: none"> • $k_{eff} \geq 1.38$ 	<ul style="list-style-type: none"> • $\rho_{TRISO}(\vec{r})$ 	230.0
	a-1d	<ul style="list-style-type: none"> • $\min(PF_{total})$ 	<ul style="list-style-type: none"> • $k_{eff} \geq 1.0$ 	<ul style="list-style-type: none"> • Coolant channel shape • PF_{total} 	334.6
	a-1e	<ul style="list-style-type: none"> • $\min(T_{max})$ 	<ul style="list-style-type: none"> • $k_{eff} \geq 1.38$ 	<ul style="list-style-type: none"> • Coolant channel shape 	692.3
	a-1f	<ul style="list-style-type: none"> • $\min(PPF_{fuel})$ 	<ul style="list-style-type: none"> • $k_{eff} \geq 1.0$ 	<ul style="list-style-type: none"> • Coolant channel shape 	222.9
2	a-2a	<ul style="list-style-type: none"> • $\min(PF_{total})$ • $\min(T_{max})$ 	<ul style="list-style-type: none"> • $k_{eff} \geq 1.38$ 	<ul style="list-style-type: none"> • $\rho_{TRISO}(\vec{r})$ • PF_{total} 	1250.9
	a-2b	<ul style="list-style-type: none"> • $\min(PF_{total})$ • $\min(PPF_{fuel})$ 	<ul style="list-style-type: none"> • $k_{eff} \geq 1.38$ 	<ul style="list-style-type: none"> • $\rho_{TRISO}(\vec{r})$ • PF_{total} 	491.7
	a-2c	<ul style="list-style-type: none"> • $\min(T_{max})$ • $\min(PPF_{fuel})$ 	<ul style="list-style-type: none"> • $k_{eff} \geq 1.38$ 	<ul style="list-style-type: none"> • $\rho_{TRISO}(\vec{r})$ 	537.7
3	a-3a	<ul style="list-style-type: none"> • $\min(PF_{total})$ • $\min(PPF_{fuel})$ • $\min(T_{max})$ 	<ul style="list-style-type: none"> • $k_{eff} \geq 1.38$ 	<ul style="list-style-type: none"> • $\rho_{TRISO}(\vec{r})$ • PF_{total} 	1367.9
	a-3b	<ul style="list-style-type: none"> • $\min(PF_{total})$ • $\min(PPF_{fuel})$ • $\min(T_{max})$ 	<ul style="list-style-type: none"> • $k_{eff} \geq 1.38$ 	<ul style="list-style-type: none"> • $\rho_{TRISO}(\vec{r})$ • PF_{total} • Coolant channel shape 	1830.0

All the optimization simulations are run on the Theta supercomputer at the Argonne Leadership Computing Facility [13].
 Each Theta node has 64 1.3-GHz Intel Xeon Phi 7230 processors.



AHTR One-Third Assembly Optimization Simulations



Objs [#]	Sim	Objectives	Constraints	Varying Parameters	Total Compute Cost [node-hours]
1	a-1a	• $\min(PF_{total})$	• $k_{eff} \geq 1.38$	• $\rho_{TRISO}(\vec{r})$ • PF_{total}	285.8
	a-1b	• $\min(T_{max})$	• $k_{eff} \geq 1.38$	• $\rho_{TRISO}(\vec{r})$	740.9
	a-1c	• $\min(PPF_{fuel})$	• $k_{eff} \geq 1.38$	• $\rho_{TRISO}(\vec{r})$	230.0
	a-1d	• $\min(PF_{total})$	• $k_{eff} \geq 1.0$	• Coolant channel shape • PF_{total}	334.6
	a-1e	• $\min(T_{max})$	• $k_{eff} \geq 1.38$	• Coolant channel shape	692.3
	a-1f	• $\min(PPF_{fuel})$	• $k_{eff} \geq 1.0$	• Coolant channel shape	222.9
2	a-2a	• $\min(PF_{total})$ • $\min(T_{max})$	• $k_{eff} \geq 1.38$	• $\rho_{TRISO}(\vec{r})$ • PF_{total}	1250.9
	a-2b	• $\min(PF_{total})$ • $\min(PPF_{fuel})$	• $k_{eff} \geq 1.38$	• $\rho_{TRISO}(\vec{r})$ • PF_{total}	491.7
	a-2c	• $\min(T_{max})$ • $\min(PPF_{fuel})$	• $k_{eff} \geq 1.38$	• $\rho_{TRISO}(\vec{r})$	537.7
3	a-3a	• $\min(PF_{total})$ • $\min(PPF_{fuel})$ • $\min(T_{max})$	• $k_{eff} \geq 1.38$	• $\rho_{TRISO}(\vec{r})$ • PF_{total}	1367.9
	a-3b	• $\min(PF_{total})$ • $\min(PPF_{fuel})$ • $\min(T_{max})$	• $k_{eff} \geq 1.38$	• $\rho_{TRISO}(\vec{r})$ • PF_{total} • Coolant channel shape	1830.0

AHTR One-Third Assembly Optimization Simulations



a-1a	<ul style="list-style-type: none"> $\min(PF_{total})$ 	<ul style="list-style-type: none"> $k_{eff} \geq 1.38$ 	<ul style="list-style-type: none"> $\rho_{TRISO}(\vec{r})$ PF_{total} 	285.8
a-1b	<ul style="list-style-type: none"> $\min(T_{max})$ 	<ul style="list-style-type: none"> $k_{eff} \geq 1.38$ 	<ul style="list-style-type: none"> $\rho_{TRISO}(\vec{r})$ 	740.9
a-1c	<ul style="list-style-type: none"> $\min(PPF_{fuel})$ 	<ul style="list-style-type: none"> $k_{eff} \geq 1.38$ 	<ul style="list-style-type: none"> $\rho_{TRISO}(\vec{r})$ 	230.0
a-1d	<ul style="list-style-type: none"> $\min(PF_{total})$ 	<ul style="list-style-type: none"> $k_{eff} \geq 1.0$ 	<ul style="list-style-type: none"> Coolant channel shape PF_{total} 	334.6
a-1e	<ul style="list-style-type: none"> $\min(T_{max})$ 	<ul style="list-style-type: none"> $k_{eff} \geq 1.38$ 	<ul style="list-style-type: none"> Coolant channel shape 	692.3
a-1f	<ul style="list-style-type: none"> $\min(PPF_{fuel})$ 	<ul style="list-style-type: none"> $k_{eff} \geq 1.0$ 	<ul style="list-style-type: none"> Coolant channel shape 	222.9

Simulations a-1b and a-1e demonstrate **how the input parameters $\rho_{TRISO}(\vec{r})$ and coolant channel shape respond to the minimize T_{max} objective.**

I constrained $k_{eff} \geq 1.38$ find optimal input parameters that achieve **similar performance to the FHR benchmark TRISO distribution.**

AHTR One-Third Assembly Optimization Simulations



	a-2a	<ul style="list-style-type: none">• $\min(PF_{total})$• $\min(T_{max})$ <ul style="list-style-type: none">• $k_{eff} \geq 1.38$ <ul style="list-style-type: none">• $\rho_{TRISO}(\vec{r})$• PF_{total}	1250.9
2	a-2b	<ul style="list-style-type: none">• $\min(PF_{total})$• $\min(PPF_{fuel})$ <ul style="list-style-type: none">• $k_{eff} \geq 1.38$ <ul style="list-style-type: none">• $\rho_{TRISO}(\vec{r})$• PF_{total}	491.7
	a-2c	<ul style="list-style-type: none">• $\min(T_{max})$• $\min(PPF_{fuel})$ <ul style="list-style-type: none">• $k_{eff} \geq 1.38$ <ul style="list-style-type: none">• $\rho_{TRISO}(\vec{r})$	537.7

Simulation a-2b demonstrates **how the input parameters PF_{total} and $\rho_{TRISO}(\vec{r})$ change as the minimize PF_{total} and PPF_{fuel} objectives interact.**

AHTR One-Third Assembly Optimization Simulations



	a-3a	<ul style="list-style-type: none">• $\min(PF_{total})$• $\min(PPF_{fuel})$• $\min(T_{max})$ <ul style="list-style-type: none">• $k_{eff} \geq 1.38$• $\rho_{TRISO}(\vec{r})$• PF_{total}	1367.9
3	a-3b	<ul style="list-style-type: none">• $\min(PF_{total})$• $\min(PPF_{fuel})$• $\min(T_{max})$ <ul style="list-style-type: none">• $k_{eff} \geq 1.38$• $\rho_{TRISO}(\vec{r})$• PF_{total}• Coolant channel shape	1830.0

Simulation a-3b is the **final and largest optimization problem** run for the one-third assembly model that varies all input parameters to optimize for all objectives.

AHTR One-Third Assembly Simulation a-1b Results



Simulation a-1b: I vary a, b, c, d, e f ($\rho_{TRISO}(\vec{x}, \vec{y})$) to minimize T_{max} .

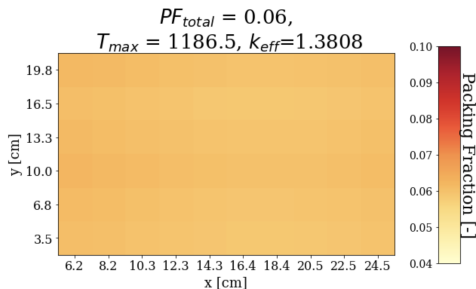
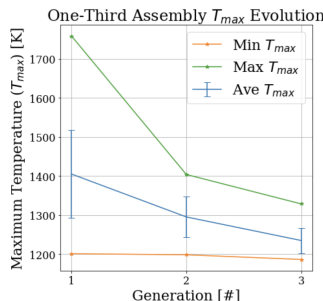


Figure 15: Simulation a-1b T_{max} evolution and TRISO distribution with lowest T_{max} .

AHTR One-Third Assembly Simulation a-1b Results



Simulation a-1b: I vary a, b, c, d, e f ($\rho_{TRISO}(\vec{x}, \vec{y})$) to minimize T_{max} .

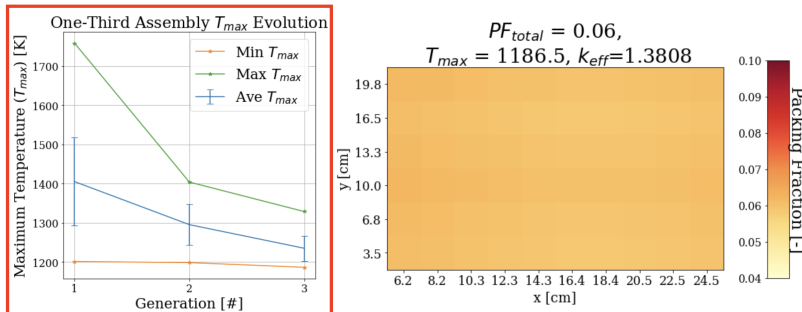


Figure 15: Simulation a-1b T_{max} evolution and TRISO distribution with lowest T_{max} .

Simulation a-1b runs for 3 generations with 128 reactor models per generation, the average T_{max} decreased by $\approx 100\text{K}$ per generation.

The average one-third assembly T_{max} converged to $\approx 1220\text{K}$.

AHTR One-Third Assembly Simulation a-1b Results



Simulation a-1b: I vary a, b, c, d, e f ($\rho_{TRISO}(\vec{x}, \vec{y})$) to minimize T_{max} .

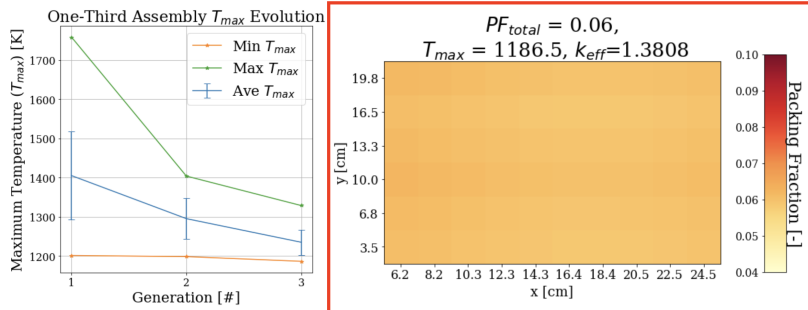


Figure 15: Simulation a-1b T_{max} evolution and TRISO distribution with lowest T_{max} .

The TRISO distribution in the final generation with the lowest T_{max} has $T_{max} = 1186\text{K}$ and an almost constant TRISO packing fraction distribution.

AHTR One-Third Assembly Simulation a-1b Results



Simulation a-1b: I vary a, b, c, d, e f ($\rho_{TRISO}(\vec{x}, \vec{y})$) to minimize T_{max} .

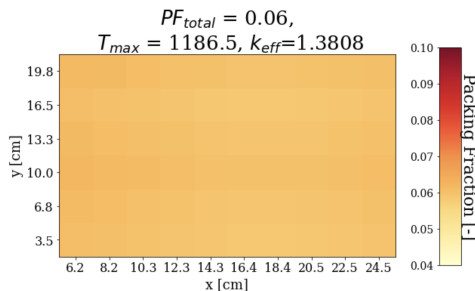
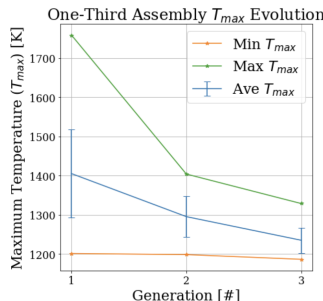


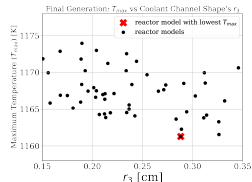
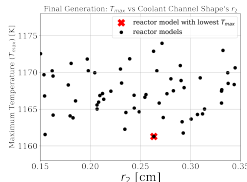
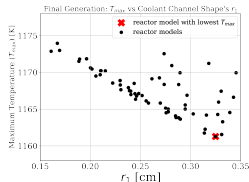
Figure 15: Simulation a-1b T_{max} evolution and TRISO distribution with lowest T_{max} .

A flatter TRISO distribution minimizes T_{max} .

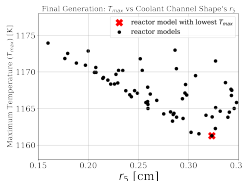
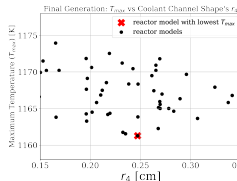
AHTR One-Third Assembly Simulation a-1e Results



I vary r_1, r_2, r_3, r_4, r_5 (coolant channel shape) to minimize T_{max} .



(a) Plot of T_{max} against r_1 . (b) Plot of T_{max} against r_2 . (c) Plot of T_{max} against r_3 .



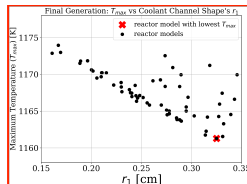
(d) Plot of T_{max} against r_4 . (e) Plot of T_{max} against r_5 .

Plots demonstrate if T_{max} is correlated with each radius values.

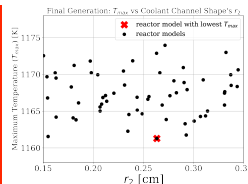
AHTR One-Third Assembly Simulation a-1e Results



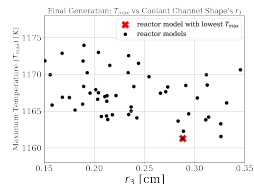
I vary r_1, r_2, r_3, r_4, r_5 (coolant channel shape) to minimize T_{max} .



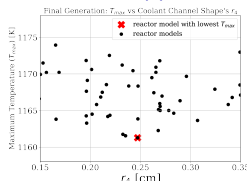
(a) Plot of T_{max} against r_1 .



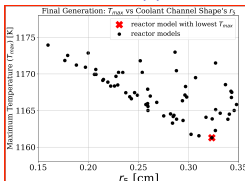
(b) Plot of T_{max} against r_2 .



(c) Plot of T_{max} against r_3 .



(d) Plot of T_{max} against r_4 .



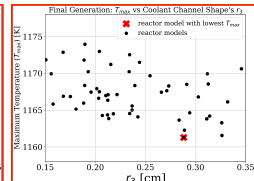
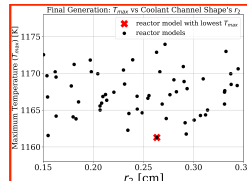
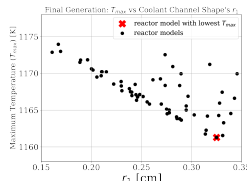
(e) Plot of T_{max} against r_5 .

There is a strong negative linear correlation between T_{max} and r_1 and r_5 .

AHTR One-Third Assembly Simulation a-1e Results



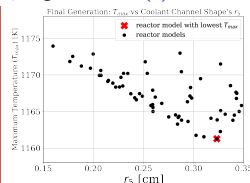
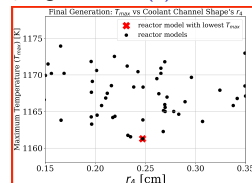
I vary r_1, r_2, r_3, r_4, r_5 (coolant channel shape) to minimize T_{max} .



(a) Plot of T_{max} against r_1 .

(b) Plot of T_{max} against r_2 .

(c) Plot of T_{max} against r_3 .



(d) Plot of T_{max} against r_4 .

(e) Plot of T_{max} against r_5 .

Random scattering shows that T_{max} has a weak correlation with r_2, r_3, r_4 .

AHTR One-Third Assembly Simulation a-1e Results

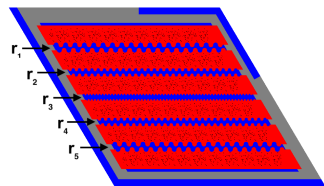
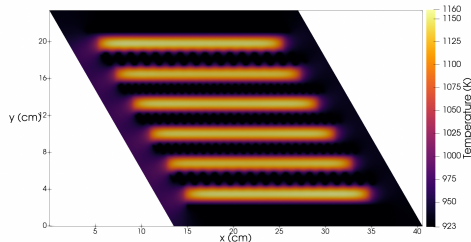


Figure 17: Temperature Distribution in the reactor model with the lowest T_{max} .

To minimize T_{max} , ROLLO maximized r_1 and r_5 to enable enhanced cooling in the top and bottom planks where the temperature peaking was occurring.

AHTR One-Third Assembly Simulation a-1e Results

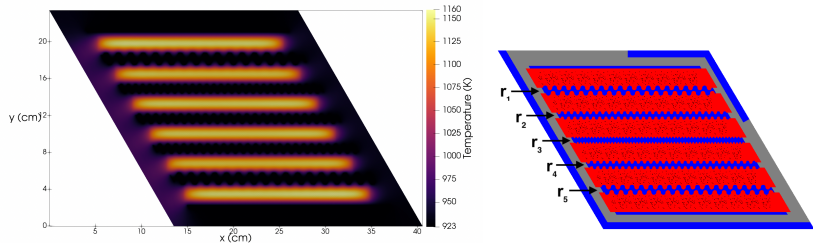


Figure 17: Temperature Distribution in the reactor model with the lowest T_{max} .

To minimize T_{max} , ROLLO maximized r_1 and r_5 to enable enhanced cooling in the top and bottom planks where the temperature peaking was occurring.

FLiBe channels located closest to temperature peaks shows a negative correlation with T_{max} .

Single-Objective Optimization Major Takeaways



Minimize PF_{total} Objective

- Driven by maximizing total fission reaction rate
- Influences oscillations in TRISO's spatial distribution
- No correlation with coolant channel shape

Single-Objective Optimization Major Takeaways



Minimize PF_{total} Objective

- Driven by maximizing total fission reaction rate
- Influences oscillations in TRISO's spatial distribution
- No correlation with coolant channel shape

Minimize T_{max} Objective

- The minimize T_{max} objective prefers a flatter TRISO distribution
- FLiBe channels located closest to temperature peaks shows a negative correlation with T_{max}



Single-Objective Optimization Major Takeaways

Minimize PF_{total} Objective

- Driven by maximizing total fission reaction rate
- Influences oscillations in TRISO's spatial distribution
- No correlation with coolant channel shape

Minimize T_{max} Objective

- The minimize T_{max} objective prefers a flatter TRISO distribution
- FLiBe channels located closest to temperature peaks shows a negative correlation with T_{max}

Minimize PPF_{fuel} Objective

- Driven by flattening thermal flux distribution
- Influences oscillations in TRISO's spatial distribution
- No correlation with coolant channel shape

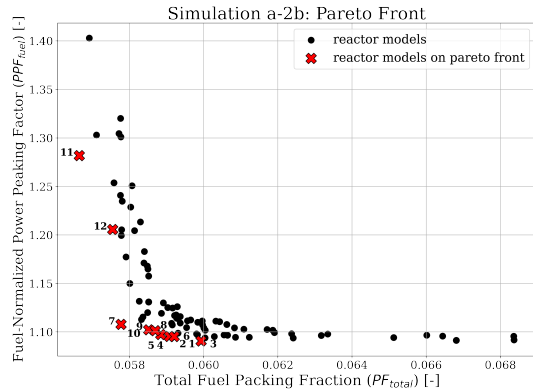
AHTR One-Third Assembly Simulation a-2b Results



Simulation a-2b

- I vary PF_{total} and $\mathbf{a}, \mathbf{b}, \mathbf{c}, \mathbf{d}, \mathbf{e} \mathbf{f}$ ($\rho_{TRISO}(\vec{x}, \vec{y})$)
- Minimize PF_{total} and PPF_{fuel} objectives
- 5 generations
- 128 reactor models per gen
- Total runtime: 492 Theta node-hours

Simulation a-2b's Pareto front shows the tradeoff between minimize PF_{total} and PPF_{fuel} objectives.

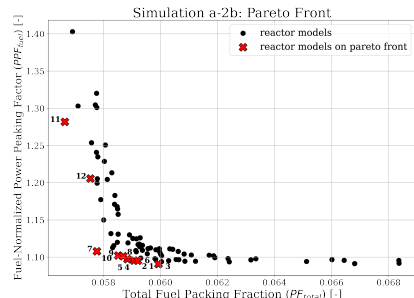


AHTR One-Third Assembly Simulation a-2b Results

Pareto Front

- Multi objective optimization with competing objectives will return **multiple optimal solutions that meet each objective to varying degrees**
- For each reactor model on the Pareto front, **none of the objective values can be improved without degrading another**

Successful multi-objective optimization finds a wide spread of reactor models on their Pareto fronts



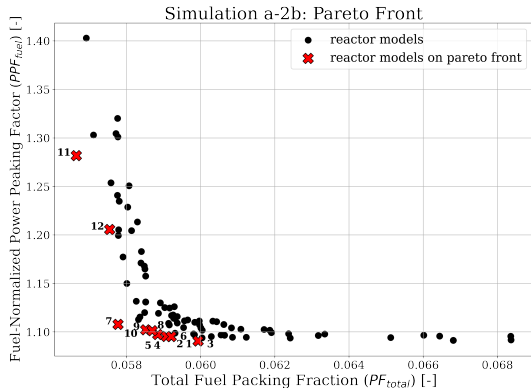
AHTR One-Third Assembly Simulation a-2b Results



Simulation a-2b

- The 12 reactor models on simulation a-2b's Pareto front have different PF_{total} and $\rho_{TRISO}(\vec{r})$ depending on extent each objective is minimized.
- Reactor 11 = lowest PF_{total} , highest PPF_{fuel}
- Reactor 3 = lowest PPF_{fuel} , highest PF_{total}
- Reactor 5 = minimizes both objectives equally

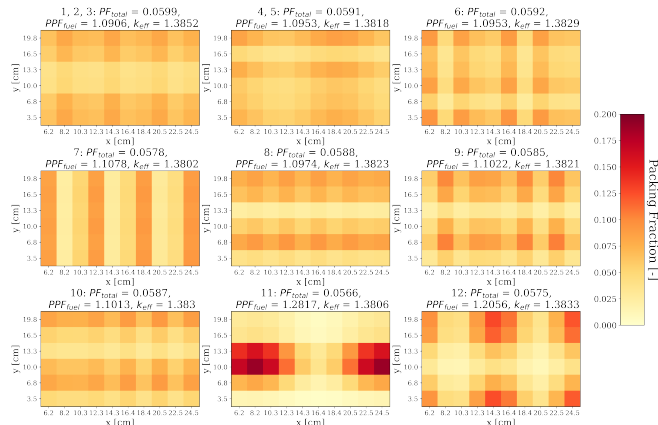
Simulation a-2b's Pareto front shows the tradeoff between minimize PF_{total} and PPF_{fuel} objectives.



AHTR One-Third Assembly Simulation a-2b Results



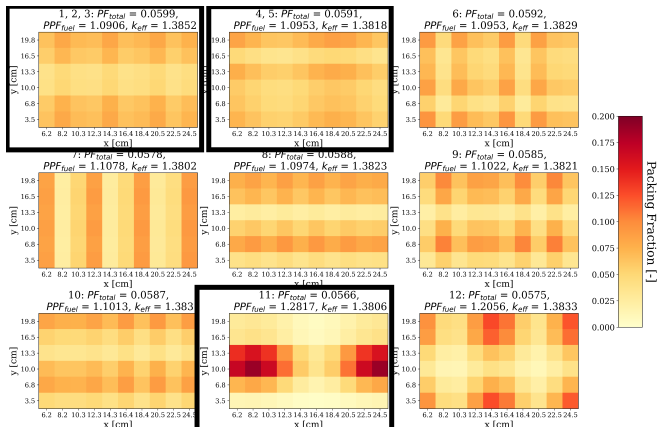
ROLLO found a wide variety of TRISO distributions on the Pareto front that minimize each objective to a different extent.



AHTR One-Third Assembly Simulation a-2b Results



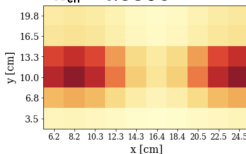
ROLLO found a wide variety of TRISO distributions on the Pareto front that minimize each objective to a different extent.



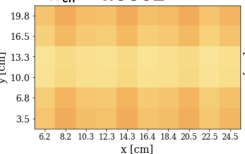
AHTR One-Third Assembly Simulation a-2b Results



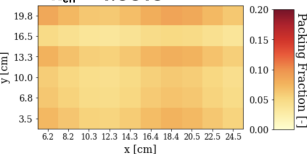
11 Lowest $PF_{total} = 0.056$
Highest $PPF_{fuel} = 1.281$
 $k_{eff} = 1.3806$



3 Lowest $PPF_{fuel} = 1.090$
Highest $PF_{total} = 0.059$
 $k_{eff} = 1.3852$



5 Equally Minimized
 $PF_{total} = 0.059, PPF_{fuel} = 1.095$
 $k_{eff} = 1.3818$



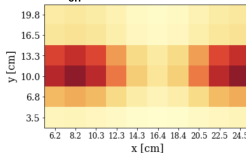
Minimize PF_{total} is driven by **maximizing total fission reaction rate**

- Reactor 11 with $PF_{total} = 0.056$ and reactor model 5 with $PF_{total} = 0.059$ have the similar k_{eff} and total fission reaction rate

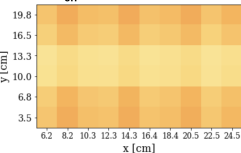
AHTR One-Third Assembly Simulation a-2b Results



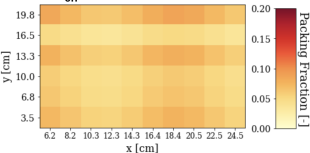
(11) Lowest $PF_{total} = 0.056$
 Highest $PPF_{fuel} = 1.281$
 $k_{eff} = 1.3806$



(3) Lowest $PPF_{fuel} = 1.090$
 Highest $PF_{total} = 0.059$
 $k_{eff} = 1.3852$



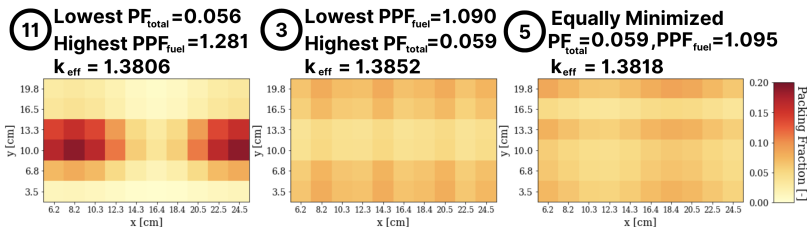
(5) Equally Minimized
 $PF_{total} = 0.059, PPF_{fuel} = 1.095$
 $k_{eff} = 1.3818$



Minimize PF_{total} is driven by **maximizing total fission reaction rate**

- Reactor 11 with $PF_{total} = 0.056$ and reactor model 5 with $PF_{total} = 0.059$ have the similar k_{eff} and total fission reaction rate
- Reactor 11 TRISO distribution enables it to achieve the same k_{eff} as reactor 5 despite having a lower PF_{total}

AHTR One-Third Assembly Simulation a-2b Results



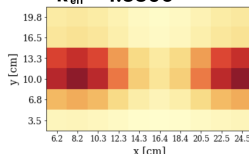
Minimize PF_{total} is driven by **maximizing total fission reaction rate**

- Reactor 11 with $PF_{total} = 0.056$ and reactor model 5 with $PF_{total} = 0.059$ have the similar k_{eff} and total fission reaction rate
- Reactor 11 TRISO distribution enables it to achieve the same k_{eff} as reactor 5 despite having a lower PF_{total}
- **Reactor 11 TRISO distribution minimizes spatial self-shielding effects**

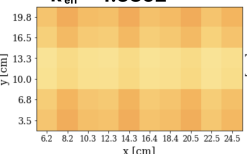
AHTR One-Third Assembly Simulation a-2b Results



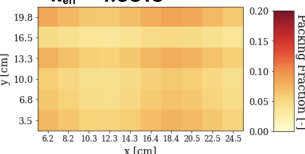
(11) Lowest $PF_{total} = 0.056$
Highest $PPF_{fuel} = 1.281$
 $k_{eff} = 1.3806$



(3) Lowest $PPF_{fuel} = 1.090$
Highest $PF_{total} = 0.059$
 $k_{eff} = 1.3852$



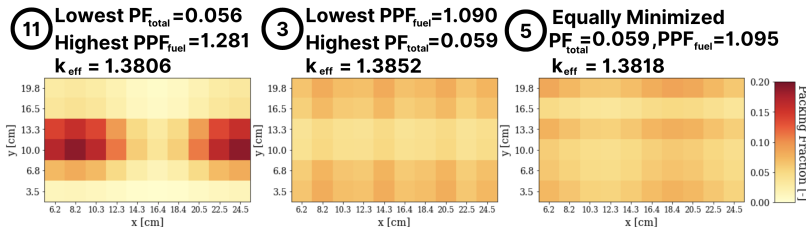
(5) Equally Minimized
 $PF_{total} = 0.059, PPF_{fuel} = 1.095$
 $k_{eff} = 1.3818$



Minimize PPF_{fuel} objective is driven by **flattening thermal flux distribution**

- Flattest to least flat thermal flux: reactor model 3 → 5 → 11
- **Reactor model 3 with lowest PPF_{fuel} has flattest flux**

AHTR One-Third Assembly Simulation a-2b Results



Minimize PPF_{fuel} objective is driven by **flattening thermal flux distribution**

- Flattest to least flat thermal flux: reactor model 3 → 5 → 11
- **Reactor model 3 with lowest PPF_{fuel} has flattest flux**

Minimize PF_{total} and Minimize PPF_{fuel} objectives influence each other resulting in **unexpected TRISO distributions at different PF_{total} values.**

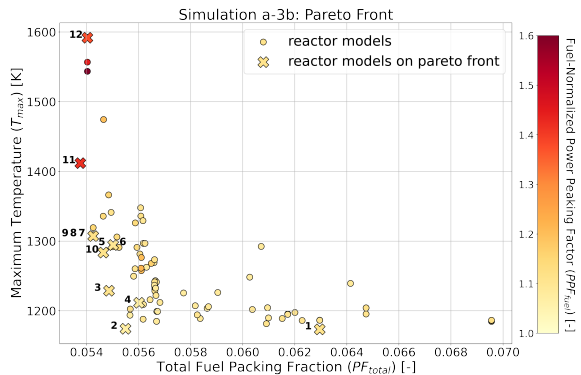
AHTR One-Third Assembly Simulation a-3b Results



Simulation a-3b

- Vary PF_{total} , a , b , c , d , e f ($\rho_{TRISO}(\vec{x}, \vec{y})$), and r_1, r_2, r_3, r_4, r_5 (coolant channel shape)
- Minimize all three objectives: PF_{total} , T_{max} and PPF_{fuel} .
- 6 generations
- 128 reactor models per gen
- Total runtime: 1528 Theta node-hours

ROLLO successfully found 12 widely spread out reactor models on a-3b's Pareto front.

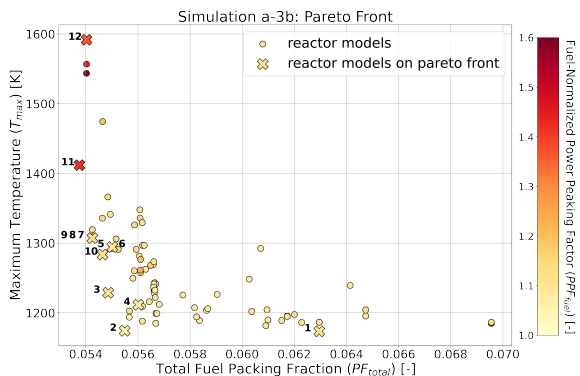


AHTR One-Third Assembly Simulation a-3b Results



Simulation a-3b

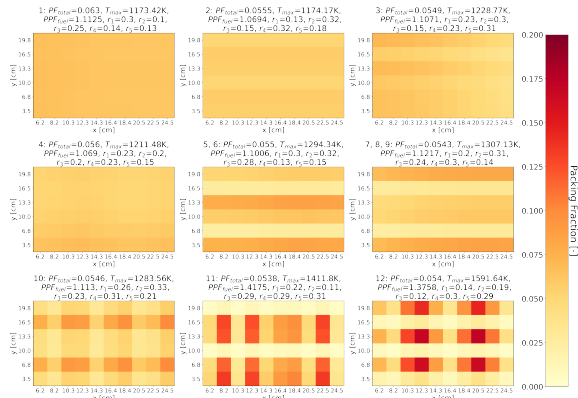
- The 12 reactor models on simulation a-3b's Pareto front have different input parameters depending on **extent each objective is minimized**
- Reactor 11 = lowest PF_{total}
- Reactor 1 = lowest T_{max}
- Reactor 4 = lowest PPF_{fuel}
- Reactor 2 = minimizes all objectives equally



AHTR One-Third Assembly Simulation a-3b Results



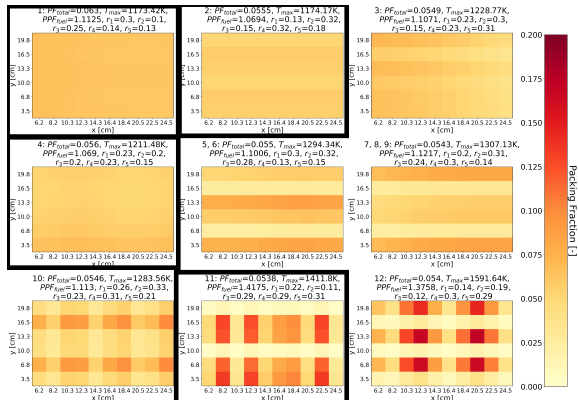
ROLLO found a wide variety of TRISO distr and coolant channel shapes on the Pareto front that minimize each objective to different extents.



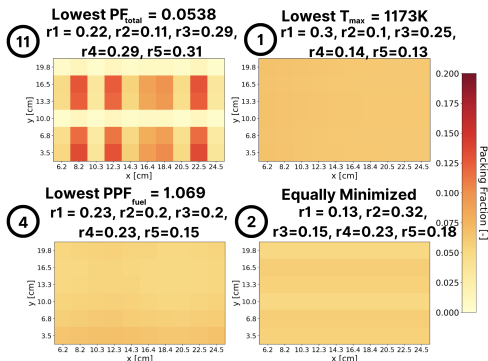
AHTR One-Third Assembly Simulation a-3b Results



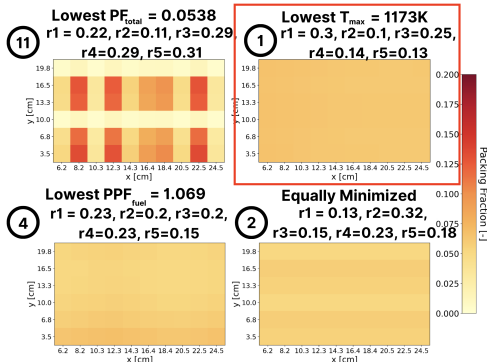
ROLLO found a wide variety of TRISO distr and coolant channel shapes on the Pareto front that minimize each objective to different extents.



AHTR One-Third Assembly Simulation a-3b Results



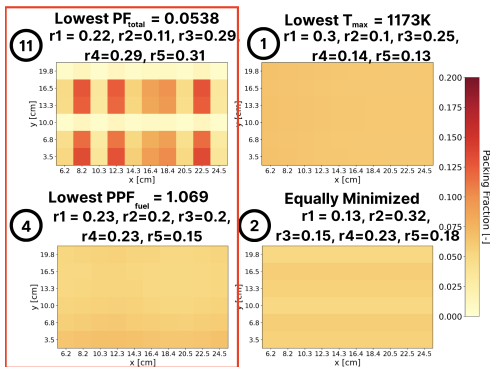
AHTR One-Third Assembly Simulation a-3b Results



Key Observations

- TRISO distribution flatness is influenced by minimize T_{max} objective

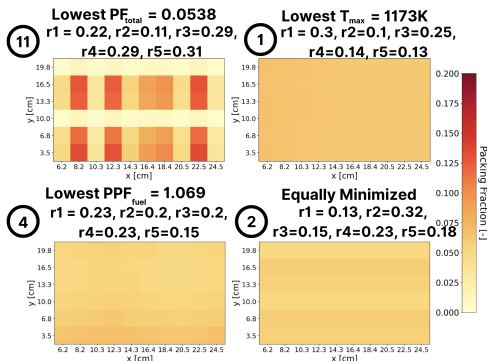
AHTR One-Third Assembly Simulation a-3b Results



Key Observations

- TRISO distribution flatness is influenced by minimize T_{max} objective
- Variations in TRISO distributions are influenced by minimize PF_{total} and PPF_{fuel} objectives

AHTR One-Third Assembly Simulation a-3b Results



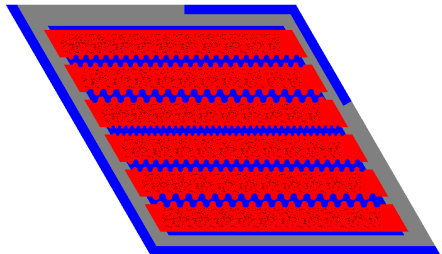
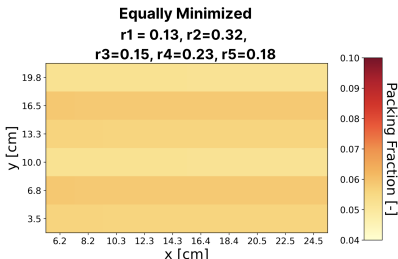
Key Observations

- TRISO distribution flatness is influenced by minimize T_{max} objective
- Variations in TRISO distributions are influenced by minimize PF_{total} and PPF_{fuel} objectives
- Larger radius values are observed near temperature peaks

AHTR One-Third Assembly Simulation a-3b Results



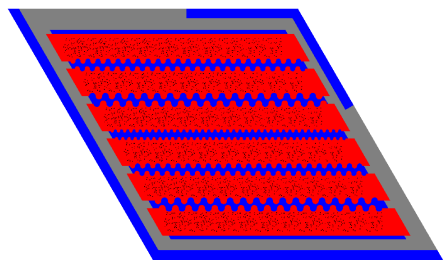
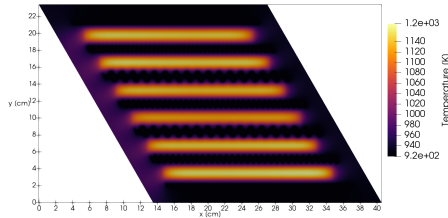
Simulation a-3b: One-third assembly model that equally minimized all objectives (reactor model 2).



AHTR One-Third Assembly Simulation a-3b Results



Simulation a-3b: One-third assembly model that equally minimized all objectives (reactor model 2).



Multi-Objective Optimization Major Takeaways

The multi-objective optimization simulations successfully explored the large design space by finding **wide spread of reactor models on their Pareto fronts.**



Multi-Objective Optimization Major Takeaways



The multi-objective optimization simulations successfully explored the large design space by finding **wide spread of reactor models on their Pareto fronts**.

The reactor models on the Pareto fronts have **different PF_{total} , TRISO distributions, and coolant channel shapes**, depending on the extent each objective is minimized due to the nature of multi-objective optimization that results in a **tradeoff between objectives**.



Multi-Objective Optimization Major Takeaways

The multi-objective optimization simulations successfully explored the large design space by finding **wide spread of reactor models on their Pareto fronts**.

The reactor models on the Pareto fronts have **different PF_{total} , TRISO distributions, and coolant channel shapes**, depending on the extent each objective is minimized due to the nature of multi-objective optimization that results in a **tradeoff between objectives**.

Minimize T_{max} objective

- Continues to flatten TRISO distribution
- Maximize radius values of Flibe channels located near temperature peaks
- TRISO distribution has a larger impact on T_{max} than coolant channel shape



Multi-Objective Optimization Major Takeaways

The multi-objective optimization simulations successfully explored the large design space by finding **wide spread of reactor models on their Pareto fronts**.

The reactor models on the Pareto fronts have **different PF_{total} , TRISO distributions, and coolant channel shapes**, depending on the extent each objective is minimized due to the nature of multi-objective optimization that results in a **tradeoff between objectives**.

Minimize T_{max} objective

- Continues to flatten TRISO distribution
- Maximize radius values of Flibe channels located near temperature peaks
- TRISO distribution has a larger impact on T_{max} than coolant channel shape

Minimize PF_{total} and PPF_{fuel} objectives

- Influences variation in TRISO spatial distributions
- These two objectives influence each other to have unexpected TRISO distributions at different PF_{total} values

ROLLO Tool + AHTR Optimization Simulations: Summary



I Successfully Completed AHTR Optimization for Non-conventional Designs Research Objectives

- I developed Reactor evOLutionary aLgorithm Optimizer (ROLLO) tool that enables generative reactor design optimization with evolutionary algorithms
- I demonstrated ROLLO's application on AHTR optimization for spatially variant fuel distributions and wavy coolant channels

ROLLO Tool + AHTR Optimization Simulations: Summary



I Successfully Completed AHTR Optimization for Non-conventional Designs Research Objectives

- I developed Reactor evOLutionary aLgorithm Optimizer (ROLLO) tool that enables generative reactor design optimization with evolutionary algorithms
- I demonstrated ROLLO's application on AHTR optimization for spatially variant fuel distributions and wavy coolant channels

Major Takeaways

- Results demonstrate ROLLO's success in conducting a multi-objective global search of the large AHTR design space to find optimal reactor models that satisfy all the objectives
- Once the ROLLO search is complete, reactor designers gain a better intuition of the model's reactor physics and can view the narrower reactor design space that meets their defined objectives



Outline

① Introduction

Overview

Background: Advanced High Temperature Reactor

Objectives: AHTR Model Development

Background: Generative Reactor Design Optimization

Objectives: AHTR Optimization for Non-Conventional Designs

Summary

② FHR Benchmark Results

FHR Benchmark Specifications

FHR Benchmark Results

③ AHTR Temperature Model Verification and Results

AHTR Temperature Model with Moltres

Key Neutronics Parameters Verification

AHTR Temperature Model Results

Summary

④ ROLLO: Reactor evOLutionary aLgorithm Optimizer

ROLLO: Reactor evOLutionary aLgorithm Optimizer

⑤ AHTR Optimization for Non-Conventional Designs

Optimization Methodology

AHTR One-Third Assembly Optimization Results

⑥ Conclusion

Conclusion

Future Work

Conclusion



FHR Benchmark and AHTR Temperature Model

Relevance

- The triple heterogeneity introduced by the geometrically complex fuel assembly design makes accurate reactor physics simulations challenging



Conclusion

FHR Benchmark and AHTR Temperature Model

Relevance

- The triple heterogeneity introduced by the geometrically complex fuel assembly design makes accurate reactor physics simulations challenging

Results Presented

- FHR benchmark Phase I-A and I-B results
- AHTR full assembly temperature model

Conclusion



FHR Benchmark and AHTR Temperature Model

Relevance

- The triple heterogeneity introduced by the geometrically complex fuel assembly design makes accurate reactor physics simulations challenging

Results Presented

- FHR benchmark Phase I-A and I-B results
- AHTR full assembly temperature model

Major Takeaways

- AHTR has passive safety behavior with negative temperature coefficients
- Increased fuel packing does not always correspond with increased k_{eff} due to self-shielding effects
- AHTR temperature peaks in the fuel stripes near the spacers
- FHR benchmark results gives confidence to the AHTR base model's accuracy

Conclusion



FHR Benchmark and AHTR Temperature Model

Relevance

- The triple heterogeneity introduced by the geometrically complex fuel assembly design makes accurate reactor physics simulations challenging

Results Presented

- FHR benchmark Phase I-A and I-B results
- AHTR full assembly temperature model

Major Takeaways

- AHTR has passive safety behavior with negative temperature coefficients
- Increased fuel packing does not always correspond with increased k_{eff} due to self-shielding effects
- AHTR temperature peaks in the fuel stripes near the spacers
- FHR benchmark results gives confidence to the AHTR base model's accuracy

Through participation in the FHR benchmark, this dissertation contributes to **deepening our understanding of the promising AHTR technology.**

contd. Conclusion



ROLLO Tool Development and AHTR Non-Conventional Design Optimization

Relevance

- Optimization tools for generating new reactor designs enabled by 3D printing do not exist
- Few demonstrations of reactor optimization for non-conventional geometries and parameters exist

contd. Conclusion



ROLLO Tool Development and AHTR Non-Conventional Design Optimization

Relevance

- Optimization tools for generating new reactor designs enabled by 3D printing do not exist
- Few demonstrations of reactor optimization for non-conventional geometries and parameters exist

Results Presented

- Reactor evOLutionary aLgorithm Optimizer (ROLLO) tool
- AHTR Optimization for heterogeneous fuel distributions and wavy coolant channels

contd. Conclusion



ROLLO Tool Development and AHTR Non-Conventional Design Optimization

Relevance

- Optimization tools for generating new reactor designs enabled by 3D printing do not exist
- Few demonstrations of reactor optimization for non-conventional geometries and parameters exist

Results Presented

- Reactor evOLutionary aLgorithm Optimizer (ROLLO) tool
- AHTR Optimization for heterogeneous fuel distributions and wavy coolant channels

Major Takeaways

- ROLLO successfully conducted multi-objective generative reactor design optimization generating optimal reactor models on a Pareto front that satisfy all the user-defined objectives

contd. Conclusion



ROLLO Tool Development and AHTR Non-Conventional Design Optimization

Relevance

- Optimization tools for generating new reactor designs enabled by 3D printing do not exist
- Few demonstrations of reactor optimization for non-conventional geometries and parameters exist

Results Presented

- Reactor evOLutionary aLgorithm Optimizer (ROLLO) tool
- AHTR Optimization for heterogeneous fuel distributions and wavy coolant channels

Major Takeaways

- ROLLO successfully conducted multi-objective generative reactor design optimization generating optimal reactor models on a Pareto front that satisfy all the user-defined objectives

By designing the ROLLO tool and demonstrating its success in optimization of the AHTR beyond classical input parameters, this dissertation contributes to **optimization tool development for reactors of the future.**



Future Work

Potential Future Research Efforts

- ① Completion of FHR benchmark Phases I-C, II, III**
 - Continue to deepen our understanding of the promising AHTR technology
- ② ROLLO software improvements**
 - Improvements will enhance ROLLO's usability and ensure longevity
- ③ AHTR design optimization with other geometry representations**
 - Topology optimization for coolant channel shape
 - Enables further exploration of the AHTR design space
- ④ Generative reactor design that considers more multiphysics phenomena**
 - AHTR model in this work: beginning of life neutronics and temperature
 - Other multiphysics components: burnup effects, structural mechanics thermal stresses, chemistry, high-fidelity thermal-hydraulics
 - Enables further optimized reactor designs
- ⑤ Generative reactor design for other reactor types**
 - Exploration of how non-conventional geometries and fuel distributions could improve performance and safety of other reactor types



References |

- [1] K. M. Ramey and B. Petrovic, "Monte Carlo modeling and simulations of AHTR fuel assembly to support V&V of FHR core physics methods," *Annals of Nuclear Energy*, vol. 118, pp. 272–282, Aug. 2018. [Online]. Available: <https://linkinghub.elsevier.com/retrieve/pii/S0306454918301816>
- [2] B. Petrovic, K. Ramey, and I. Hill, "Benchmark Specifications for the Fluoride-salt High-temperature Reactor (FHR) Reactor Physics Calculations," Nuclear Energy Agency, Tech. Rep., Mar. 2021.
- [3] O. Mireles, "Refractory Alloy Additive Manufacture Build Optimization (RAAMBO)," in *TechConnect World Innovation Conference and Expo*, 2022.
- [4] Autodesk®, "Autodesk® Fusion 360™," 2020. [Online]. Available: <https://www.autodesk.com/products/fusion-360/overview>
- [5] P. K. Romano, N. E. Horelik, B. R. Herman, A. G. Nelson, B. Forget, and K. Smith, "OpenMC: A state-of-the-art Monte Carlo code for research and development," *Annals of Nuclear Energy*, vol. 82, no. Supplement C, pp. 90–97, Aug. 2015. [Online]. Available: <http://www.sciencedirect.com/science/article/pii/S030645491400379X>



References II

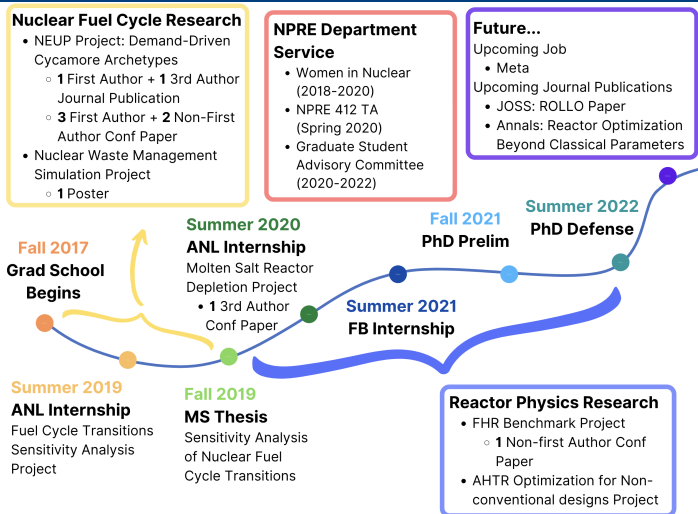
- [6] A. Lindsay, G. Ridley, A. Rykhlevskii, and K. Huff, "Introduction to Moltres: An application for simulation of Molten Salt Reactors," *Annals of Nuclear Energy*, vol. 114, pp. 530–540, Apr. 2018. [Online]. Available: <https://linkinghub.elsevier.com/retrieve/pii/S0306454917304760>
- [7] M. B. Chadwick, M. Herman, P. Obložinský, M. E. Dunn, Y. Danon, A. C. Kahler, D. L. Smith, B. Pritychenko, G. Arbanas, R. Arcilla, R. Brewer, D. A. Brown, R. Capote, A. D. Carlson, Y. S. Cho, H. Derrien, K. Guber, G. M. Hale, S. Hoblit, S. Holloway, T. D. Johnson, T. Kawano, B. C. Kiedrowski, H. Kim, S. Kunieda, N. M. Larson, L. Leal, J. P. Lestone, R. C. Little, E. A. McCutchan, R. E. MacFarlane, M. MacInnes, C. M. Mattoon, R. D. McKnight, S. F. Mughabghab, G. P. A. Nobre, G. Palmiotti, A. Palumbo, M. T. Pigni, V. G. Pronyaev, R. O. Sayer, A. A. Sonzogni, N. C. Summers, P. Talou, I. J. Thompson, A. Trkov, R. L. Vogt, S. C. van der Marck, A. Wallner, M. C. White, D. Wiarda, and P. G. Young, "ENDF/B-VII.1 Nuclear Data for Science and Technology: Cross Sections, Covariances, Fission Product Yields and Decay Data," *Nuclear Data Sheets*, vol. 112, no. 12, pp. 2887–2996, Dec. 2011.
- [8] G. Chee, "arfc/fhr-benchmark," 2021. [Online]. Available: <https://github.com/arfc/fhr-benchmark>



References III

- [9] B. Petrovic, K. Ramey, I. Hill, E. Losa, M. Elsawi, Z. Wu, C. Lu, J. Gonzales, D. Novog, and G. Chee, "Preliminary Results of the NEA FHR Benchmark Phase IA and IB (Fuel Element 2-D Benchmark)," in *The International Conference on Mathematics and Computational Methods Applied to Nuclear Science and Engineering, Raleigh, NC*, 2021.
- [10] D. Gaston, C. Newman, G. Hansen, and D. Lebrun-Grandie, "MOOSE: A parallel computational framework for coupled systems of nonlinear equations," *Nuclear Engineering and Design*, vol. 239, no. 10, pp. 1768–1778, Oct. 2009. [Online]. Available: <http://www.sciencedirect.com/science/article/pii/S0029549309002635>
- [11] C. Geuzaine and J.-F. Remacle, "Gmsh: A 3-D finite element mesh generator with built-in pre- and post-processing facilities," *International Journal for Numerical Methods in Engineering*, vol. 79, no. 11, pp. 1309–1331, 2009. [Online]. Available: <https://onlinelibrary.wiley.com/doi/abs/10.1002/nme.2579>
- [12] C. A. Gentry, "Development of a Reactor Physics Analysis Procedure for the Plank-Based and Liquid Salt-Cooled Advanced High Temperature Reactor," Ph.D. dissertation, University of Tennessee - Knoxville, 2016. [Online]. Available: https://trace.tennessee.edu/utk_graddiss/3695
- [13] "Theta/ThetaGPU," *Argonne Leadership Computing Facility*, 2022. [Online]. Available: <https://www.alcf.anl.gov/alcf-resources/theta>

Grad School Journey





Summary

AHTR Model Development for the FHR Benchmark

Results Presented

- FHR benchmark Phase I-A and I-B results
- AHTR full assembly temperature model

Through participation in the FHR benchmark, this dissertation contributes to **deepening our understanding of the promising AHTR technology**.

ROLLO Tool Development and AHTR Non-Conventional Design Optimization

Results Presented

- Reactor evOLutionary aLgorithm Optimizer (ROLLO) tool
- AHTR Optimization for heterogeneous fuel distributions and wavy coolant channels

By designing the ROLLO tool and demonstrating its success in optimization of the AHTR beyond classical input parameters, this dissertation contributes to **optimization tool development for reactors of the future**.



FHR Benchmark Specifications

UIUC participates in the benchmark with OpenMC and using the ENDF/B-VII.1 material cross section library

Table 1: OECD NEA's FHR Benchmark Phases [2].

Phases	Sub-phases	Description
Phase I: fuel assembly	I-A	2D model, steady-state
	I-B	2D model depletion
	I-C	3D model steady-state and depletion
Phase II: 3D full core	II-A	Steady-state
	II-B	Depletion
Phase III: 3D full core with feedback & multicycle analysis	III-A	Full core depletion with feedback
	III-B	Multicycle analysis

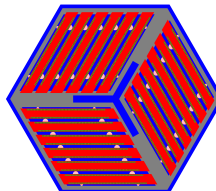


Figure 18: AHTR fuel assembly.



FHR Benchmark Specifications

Only Phase I-A and I-B specifications have been released

Table 2: Description of the Fluoride-Salt-Cooled High-Temperature Reactor benchmark Phase I-A cases [2].

Case	Description
1A	<ul style="list-style-type: none">• Reference case• 9 wt% enrichment• Hot full power• no burnable poison and control rod
2AH	<ul style="list-style-type: none">• Hot zero power
2AC	<ul style="list-style-type: none">• Cold zero power
3A	<ul style="list-style-type: none">• Control rod inserted
4A	<ul style="list-style-type: none">• Discrete europia burnable poison
4AR	<ul style="list-style-type: none">• Discrete europia burnable poison• Control rod inserted
5A	<ul style="list-style-type: none">• Integral (dispersed) europia burnable poison
6A	<ul style="list-style-type: none">• Double TRISO particle fuel
7A	<ul style="list-style-type: none">• 19.75 wt% enrichment

Benchmark participants must produce the following results for the 9 cases: k_{eff} , reactivity coefficients (β_{eff} , α_D , $\alpha_{T,FlBe}$, α_M), fission source distribution, neutron flux distribution, fuel assembly averaged neutron spectrum



FHR Benchmark Phase I-B Results

- FHR Benchmark Phase I-B: 2D assembly depletion model
- Benchmark participants are working on resolving differences in these results

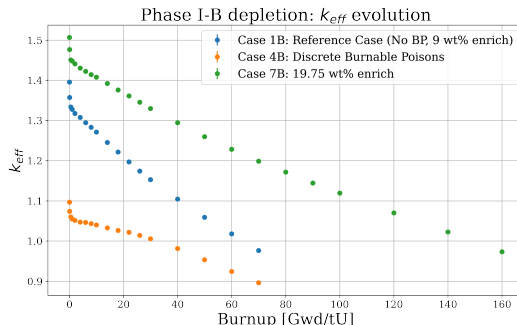


Figure 19: UIUC results: FHR Benchmark Phase I-B depletion k_{eff} evolution for Cases 1B, 4B, and 7B. Case 1B is the reference case, Case 4B is the discrete burnable poison case, and Case 7B is the 19.75% enrichment case. Error bars are included but are barely visible due to the low ~40nm uncertainty.

AHTR Temp Model k_{eff} and Reactivity Coefficients Verification



Table 3: k_{eff} and reactivity comparison.

Software	Homogenized?	k_{eff}	Diff [pcm]	Reactivity [pcm]	Reactivity Diff [pcm]
OpenMC	No	1.39850 ± 0.00126	-	28495 ± 64	-
OpenMC	Yes	1.398373 ± 0.00115	-13	28488 ± 58	-6
Moltres	Yes	1.40273	+423	28710	+216

The 13pcm k_{eff} and 6pcm reactivity diff, between continuous and homogenized OpenMC simulations are within uncertainty, showing that **selected spatial homogenizations and energy discretizations are acceptable**. The Moltres simulation shows a 423pcm diff in k_{eff} and 216pcm diff in reactivity.

Table 4: Reactivity coefficients comparison.

Software	Homogenized?	β_{eff} [pcm]	Diff [pcm]	Total $\frac{\Delta\rho}{\Delta T}$ [pcm · K ⁻¹]	Diff [pcm · K ⁻¹]
OpenMC	No	653.40	-	-3.63	-
Moltres	Yes	652.57	-0.84	-4.06	-0.43

Good agreement for Moltres' delayed neutron fraction (β_{eff}) and temperature reactivity feedback ($\frac{\Delta\rho}{\Delta T}$)

AHTR Temp Model Flux Verification

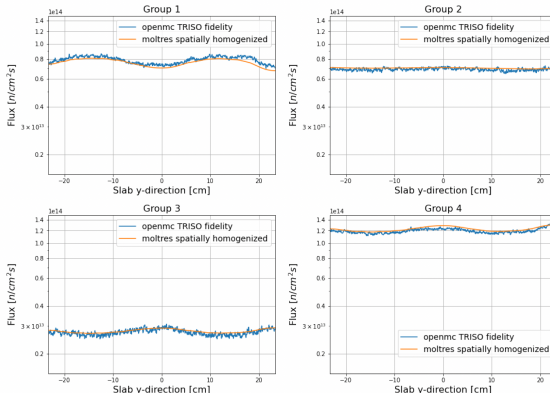


Figure 20: 4-group flux distribution comparison.

2-norm Diff [%]

- Group 1: 0.13%
- Group 2: 0.08%
- Group 3: 0.10%
- Group 4: 0.09%

Max Diff [%]

- Group 1: -10.57%
- Group 2: +7.58%
- Group 3: +8.96%
- Group 4: +6.97%

AHTR Temp Model Neutron Energy Spectrum Verification

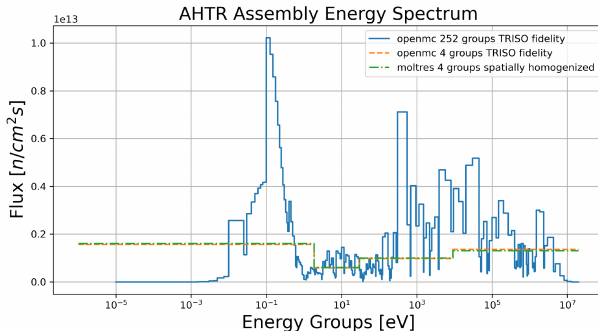


Figure 21: Neutron Energy Spectrum Comparison.

Good agreement between OpenMC and Moltres models 4-group spectrums.



TRISO Particle Homogenization

Table 5: Straightened Advanced High-Temperature Reactor (AHTR) fuel plank k_{eff} for the case with no Tristructural Isotropic (TRISO) homogenization and case with homogenization of the four outer layers. Both simulations were run on one BlueWaters supercomputer XE Node using OpenMC with 80 active cycles, 20 inactive cycles, and 8000 particles.

TRISO Homogenization	k_{eff} [-]	Simulation Time [s]
None	1.38548 ± 0.00124	233
Four outer layers	1.38625 ± 0.00109	168

The TRISO particle outer four-layer homogenization resulted in a 30% speed-up without compromising accuracy with k_{eff} values within each other's uncertainty.

As a result, the homogenized models are used for all subsequent optimization efforts.



ROLLO Successfully Verified with ^{239}Pu Critical Bare Sphere

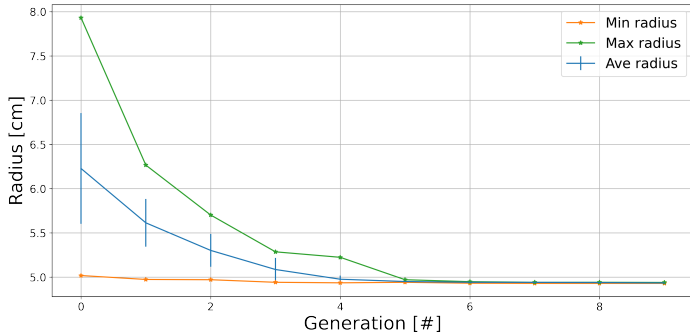


Figure 22: Results for each generation for Reactor evOLutionary aLgorithm Optimizer (ROLLO)'s genetic algorithm optimization to the find the critical radius of a ^{239}Pu bare sphere.

ROLLO successfully finds the critical radius of the ^{239}Pu bare sphere to be 4.9856cm.

ROLLO ^{239}Pu Critical Bare Sphere Input File



```

{
    "control_variables": {
        "radius": {"min": 1.0, "max": 8.0}
    },
    "evaluators": {
        "openmc": {
            "order": 0,
            "input_script": ["python", "critical_sphere.py"],
            "inputs": ["radius"],
            "outputs": ["keff", "radius"],
            "output_script": ["python", "get_sphere_keff.py"]
        }
    },
    "constraints": {"keff": {"operator": ">=", "constrained_val": [1.0]}},
    "algorithm": {
        "parallel": "multiprocessing",
        "keep_files": "none",
        "objective": ["min"],
        "optimized_variable": ["radius"],
        "pop_size": 80,
        "generations": 10
    }
}

import openmc
import numpy as np

pu = openmc.Material()
pu.set_density("g/cm3", 19.84)
pu.add_nuclide("Pu239", 1)
mats = openmc.Materials([pu])

radius = {{radius}}

fuel_sphere = openmc.Sphere(r=radius, boundary_type='vacuum')
fuel_cell = openmc.Cell(fill=pu, region=fuel_sphere)
univ = openmc.Universe(cells=[fuel_cell])
geom = openmc.Geometry(univ)

settings = openmc.Settings()
settings.batches = 100
settings.inactive = 20
settings.particles = 20000
settings.temperature = {"multipole": True, "method": "interpolation"}

mats.export_to_xml()
geom.export_to_xml()
settings.export_to_xml()
openmc.run()

```

Figure 23: ROLLO ^{239}Pu Critical Bare Sphere Input File.



AHTR Plank Geometry

A sine distribution governs TRISO packing fraction distribution:

$$\rho_{TRISO}(\vec{x}) = (\mathbf{a} \cdot \sin(\mathbf{b} \cdot x + \mathbf{c}) + 2) \cdot NF$$

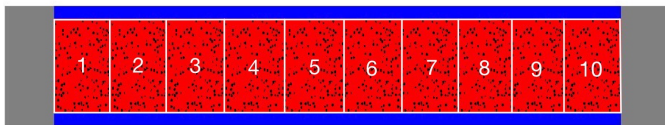


Figure 24: Straightened AHTR Plank with 10 fuel cells with random TRISO packing.

r_{top} and r_{bot} control coolant channel shape:

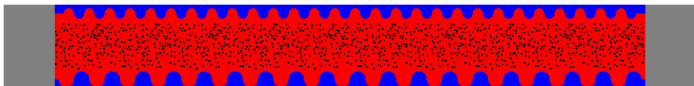


Figure 25: AHTR Plank with coolant channel shape variation, $r_{top} = 0.2\text{cm}$ and $r_{bot} = 0.3\text{cm}$.



Minimize PPF_{fuel} Driving Factor Derivation

Equation Analysis Equation 6.1 shows the relationship between fission reaction rate, flux, and material properties:

$$RR_f = \Phi \times \sigma_f \times N \quad (6.1)$$

where

RR_f = fission reaction rate [*reactions · cm⁻³ · s⁻¹*]

Φ = neutron flux [*neutrons · cm⁻² · s⁻¹*]

σ_f = microscopic cross section [*cm²*]

N = atomic number density [*atoms · cm⁻³*]

Since microscopic cross section is constant for the same fuel material, I rearrange Equation 6.1 into Equation 6.2:

$$\Phi \propto \frac{RR_f}{N} \quad (6.2)$$



Minimize PPF_{fuel} Driving Factor Derivation

In Section 5.3.3, I defined the fuel-normalized power peaking factor (PPF_{fuel}) as:

$$PPF_{fuel} = \frac{\max\left(\frac{fqr_j}{PF_j}\right)}{\text{ave}\left(\frac{fqr_j}{PF_j}\right)} \quad (6.3)$$

where

PPF_{fuel} = fuel-normalized power peaking factor

j = discretized fuel area j



Minimize PPF_{fuel} Driving Factor Derivation

fqr_j = fission-q-recoverable at position j (OpenMC tally)

PF_j = fuel packing fraction at position j

The fission reaction rate (RR_f) is proportional to fission energy production rate (fqr). The atomic number density (N) is proportional to the fuel packing fraction (PF). Thus, I can rearrange Equation 6.2 into Equation 6.4:

$$\Phi_j \propto \frac{fqr_j}{PF_j} \quad (6.4)$$

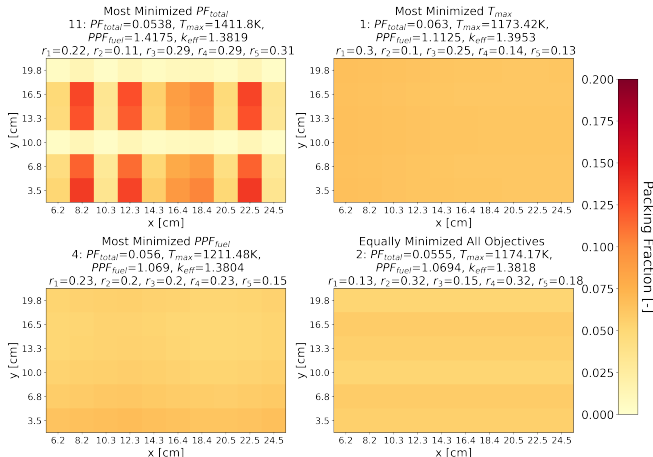
Finally, I can further rearrange Equation 6.4 into Equation 6.5:

$$\begin{aligned} \frac{\max(\Phi_j)}{\text{ave}(\Phi_j)} &\propto \frac{\max\left(\frac{fqr_j}{PF_j}\right)}{\text{ave}\left(\frac{fqr_j}{PF_j}\right)} \\ \frac{\max(\Phi_j)}{\text{ave}(\Phi_j)} &\propto PPF_{fuel} \end{aligned} \quad (6.5)$$

Appendix

Grad School Journey
 Summary
 FHR Benchmark Specifications
 Key Neutronics Parameters Verification
 TRISO Particle Homogenization
 ROLLO Verification
 Minimize PPF_{fuel} Driving Factor Derivation
 Simulation a-3b

AHTR One-Third Assembly Simulation a-3b Detailed Results





Simulation a-3b Hypervolume

Table 6: Simulation a-3b hypervolume values at each generation.

Three Objectives: Simulation a-3b	
Reference point: (0.07, 1700, 1.8)	
Generation	Hypervolume [-]
1	5.4961
2	5.6739
3	5.6876
4	5.8104
5	6.0023
6	6.0093

For each optimization, I must **balance convergence and computational cost**.

The hypervolume is calculated by finding the volume between the reference point and the objective values of the Pareto front's reactor models (bigger hypervolume = more converged solution).

I determine if convergence criteria is met by evaluating if the difference between generations' hypervolume values are getting smaller.